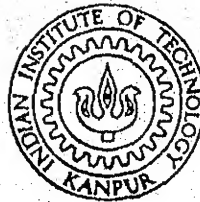


SINTERING BEHAVIOUR OF MULTICOMPONENT TITANIUM ALLOYS

by
M. SUJATA



DEPARTMENT OF METALLURGICAL ENGINEERING

INDIAN INSTITUTE OF TECHNOLOGY KANPUR

JANUARY, 1991

MIME

1991

M

SUJ

SINTERING BEHAVIOUR OF MULTICOMPONENT TITANIUM ALLOYS

A Thesis Submitted
In Partial Fulfilment of the Requirements
for the Degree of
MASTER OF TECHNOLOGY

by
M. SUJATA

to the
DEPARTMENT OF METALLURGICAL ENGINEERING
INDIAN INSTITUTE OF TECHNOLOGY KANPUR
JANUARY, 1991

1 2 APR 1991

CENTRAL LIBRARY
I. I. T., KANPUR

Acc. No. A. . 1.10759

7K


673.73225

See 6

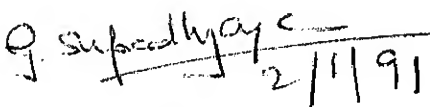
MME-1981-M-SUT-SIN.

CERTIFICATE

It is certified that the work contained in the thesis entitled "SINTERING BEHAVIOUR OF MULTICOMPONENT TITANIUM ALLOYS" has been carried out under our supervision and that this work has not been submitted elsewhere for a degree.


Dr. S. BHARGAVA
Assistant Professor

Department of Metallurgical Engineering
Indian Institute of Technology
Kanpur


Dr. G.S. UPADHYAYA
Professor

January, 1991

ACKNOWLEDGEMENTS

I express my gratitude to my supervisors Dr. G.S. Upadhyaya and Dr. S. Bhargava who have extended their valuable guidance as well as moral support to complete my thesis work successfully.

I am grateful to Mr. S.C. Soni who helped me in printing the micrographs and to my senior colleagues Mr. S.K. Bhaumik, Mr. H.N. Azari and Mr. P.K. Kar who encouraged me and helped me throughout my M.Tech. programme.

I thank Mr. P. Saha and all my friends in the hostel for their help during the preparation of this thesis.

I thank Mr. B.K. Jain, Mr. Mukherjee, Mr. Paul and Mr. Lal for their technical help and lastly Mr. R.N. Srivastava for his typing.

TABLE OF CONTENTS

	Page
CHAPTER 1. INTRODUCTION	1
CHAPTER 2. POWDER METALLURGY OF TITANIUM ALLOYS - A REVIEW	6
2.1. Preparation of Powders of Titanium and its Alloys	6
2.1.1. Sponge Fine Production Process	6
2.1.2. Rotating Electrode Process	8
2.1.3. Hydride Dehydride Process	9
2.1.4. Rapid Solidification Process	9
2.2. Consolidation of Powders	9
2.2.1. Consolidation of Elemental Powders	10
2.2.1.1. Cold Pressing and Sintering	10
2.2.1.2. Slip Casting/Gravity Moulding	12
2.2.1.3. Forging/Rolling/Extrusion	12
2.2.2. Consolidation of Prealloyed Powders	13
2.2.2.1. Hot Isostatic Pressing (HIP)	13
2.2.2.2. Rolling/Forging/Extrusion	14
2.2.3. Consolidation of Rapidly Solidified Powders	15
2.3. Transient Liquid Phase Sintering (TLPS)	15
CHAPTER 3. AIMS OF THE PRESENT INVESTIGATION	16
CHAPTER 4. EXPERIMENTAL PROCEDURE	17
4.1. Powder Characteristics	17
4.2. Particle Size Analysis of Powders	20
4.3. Observation of Powder Morphology	20
4.4. Premix Preparation	21
4.5. Compaction	21
4.6. Sintering	21
4.7. Hot Isostatic Pressing	22
4.8. Heat Treatment	22
4.8.1. Homogenizing of Ti-6 Al-6 V-xSn Alloys	23
4.8.2. Solution Treating/Overaging (STOA) and Mill Annealing of HIP'ed Ti-6 Al-4 V	23
4.8.2.1. STOA Treatment	23
4.8.2.2. Mill Annealing	23
4.9. Evaluation of Sintered Properties	24
4.9.1. Density and Porosity Measurements	24
4.9.2. Determination of Total Porosity and Pore Size Distribution	25
4.9.3. Hardness Measurements	25
4.9.3.1. Macrohardness	25
4.9.3.2. Microhardness	25
4.10. Microstructural Examination	26
4.10.1. Optical Microscopy	26
4.10.2. Scanning Electron Microscopy	26
4.11. Fractography	27

	Page
CHAPTER 5. RESULTS	28
5.1. Transient Liquid Phase Sintered α -Titanium Alloys	28
5.1.1. Densification	28
5.1.2. Microstructure and Pore Characteristics	29
5.1.3. Hardness of Alloys	31
5.2. Transient Liquid Phase Sintered $\alpha + \beta$ Titanium Alloys	33
5.2.1. Densification	33
5.2.2. Microstructural Development	33
5.2.3. Hardness of Alloys	35
5.3. HIP'ed $\alpha + \beta$ Titanium Alloy	35
CHAPTER 6. DISCUSSION	38
6.1. Transient Liquid Phase Sintering of Ti-Al, Ti-Sn and Ti-Al-Sn Alloys	38
6.1.1. Densification	38
6.1.2. Microstructural Development	43
6.1.3. Hardness of the Alloys	44
6.2. Transient Liquid Phase Sintering of Ti-6 Al-6 V-xSn ($x = 0, 1, 2, 3$) Alloys	45
6.2.1. Densification	45
6.2.2. Microstructural Development	46
6.2.3. Hardness of the Alloys	48
6.3. HIP'ing of Ti-6 Al-4 V Alloy	48
CHAPTER 7. CONCLUSIONS	50
REFERENCES	52

SYNOPSIS

The transient liquid phase sintering behaviour of binary and ternary alpha alloys of titanium belonging to Ti-Al-Sn and alpha-beta alloys of titanium belonging to Ti-Al-V-Sn systems has been studied. Compacts of various Ti-Sn, Ti-Al, Ti-Al-Sn and Ti-Al-V-Sn alloys were prepared from the premixed elemental powders and were vacuum sintered. Characterization of sintered alloys consisted of measurements of sintered density, interconnected and closed porosities, pore size distribution, grain size, hardness and microhardness and examination of the microstructure by optical as well as scanning electron microscopy. Sintered density and hardness of different alloys were found to increase with increasing alloying additions. The combined effect of tin and aluminium in ternary alloys was found to be positively skewed with most of the pores being finer than 20 μm . Interconnected porosity in both binary and ternary alpha alloys was found to be increasing with increasing the tin content of alloys. In the case of alpha-beta titanium alloys, both tin content and increase in sintering temperature were found to enhance sinterability. Different homogenizing treatments were given for developing a uniform microstructure in alpha-beta alloys obtained by their transient liquid phase sintering. For the prealloyed Ti-6 Al-4 V powder, hot isostatic pressing above the beta-transus temperature was carried out in order to get a fully dense material. Effect of various heat treatments on the microstructure and mechanical properties of

hot isostatically pressed Ti-6 Al-4 V alloy was studied. Results obtained have been discussed in terms basic alloy characteristics of Ti-Al, Ti-Sn, Ti-Al-Sn and Ti-Al-V-Sn systems and a good correlation between them and theoretical considerations has been pointed out.

CHAPTER - 1

INTRODUCTION

An excellent resistance to corrosion in most chemical environments and a high specific strength make titanium alloys highly suitable for many commercial applications. Various titanium alloys have, therefore, been developed which offer a wide range of properties [1]. Depending on their chemical composition these alloys have been classified into three general categories, viz. α , $\alpha + \beta$ and β alloys. Pure titanium is polymorphic and undergoes an allotropic transformation from low temperature hcp phase α to a high temperature bcc phase β as its temperature is raised through 882.5°C . Alloying elements which, when dissolved in titanium, raise its polymorphic transformation temperature are classified as α -stabilizers. Aluminium, gallium, oxygen, nitrogen and carbon are the alloying elements falling in this category. Alloying elements such as tin and zirconium do not affect the polymorphic transformation temperature of titanium in any significant ways and therefore are considered as "neutral" elements. However, since they preferably dissolve in α -phase, they are also sometimes considered as α -stabilizers. On the other hand, alloying elements which lower the polymorphic transformation temperature of titanium are known as β -stabilizers. Vanadium, molybdenum, chromium, iron, manganese, copper and hydrogen are important β -stabilizing elements often added in titanium alloys.

Titanium alloys in which only α -stabilizers are added become solid solution strengthened and possesses a single phase structure consisting of α -phase only. They are known as α -alloys. Alloys, in which both α and β stabilizers are added as alloying elements stabilize both α and β phases at room temperature and are known as $\alpha + \beta$ titanium alloys. Finally when β -stabilizing elements in titanium are added in large quantities so that the bcc β phase is stabilized at room temperature, the alloys so developed are classified as β -alloys. $\alpha + \beta$ alloys of titanium, depending on the volume fractions of stabilized α or β phases, are further classified as near α or near β alloys. Some of the prominent alloys along with their chemical compositions and major applications have been shown in Table 1.1.

Majority of the components made from titanium alloy are manufactured by forging. Hot deformation processing of titanium alloys, in general, requires the heating of the work piece material to a temperature of 850-1050°C, i.e. to a temperature corresponding to the upper region of the two phase $\alpha + \beta$ field, so that the material after its working possesses the desirable distribution of its microstructural features. Since dies in conventional forging processes are heated to a maximum temperature of 450°C, die-chilling of the work piece in such cases cannot be avoided. However, the flow stress of titanium alloys is very sensitive to temperature and strain rate in the hot forging range, particularly below the β -transus temperature. Due to this reason, severe microstructural inhomogeneities can arise by die chilling of work piece surfaces in conventional forging processes [2,3]. Though, in principle, this can be

TABLE 1.1. Applications of some important titanium alloys

Alloy	Applications
<u>α-alloys</u>	
CP Titanium	Skins for aircraft webs and stiffeners, fire walls, engine rings and fasteners
Ti-5 Al	Cryogenic applications
Ti-5 Al-2.5 Sn	Liquid nitrogen tanks, high pressure vessels
<u>α-β alloys</u>	
Ti-6 Al-4 V	Automobile engine components, pump impellers, steam turbine blades
Ti-6 Al-6 V-2 Sn	Aerospace and automobile engine components and engine mount supports
<u>β-alloys</u>	
Ti-50 Nb	Super-conductors
Ti-13 V-11 Cr-3 Al	High temperature applications, forged components

avoided by forging a component through a series of preforming and blocking operations the high cost of dies generally prohibits the adoption of such a processing route. It is therefore invariably economically viable to leave a large machining envelope around a forged component [2], making the material utilization factor (MUF) in manufacturing a component from titanium alloys very low. Titanium alloys therefore cannot be exploited for many commercial applications in proportion to their vast potential. It is not surprising therefore that a considerable effort has been put towards the development of net shape or near-net shape technologies for titanium alloys.

P/M processes, in general, constitute an important group of net shape/near net shape processes. It is not surprising therefore that P/M of titanium alloys has drawn the attention of researchers. In fact, powder metallurgy techniques have been used for the manufacture of titanium parts from the time titanium sponge was produced by Kroll. Gould Inc. produced titanium parts and developed a number of methods like cold pressing and sintering, isostatic pressing, slip casting, coining, hot pressing and forging of powder preforms [4]. It has been reported that powder metallurgy processes have a scrap loss of 10 to 20% compared to that of nearly 50% incurred if the part has to be manufactured by ingot metallurgy (I/M) route. These differences are even more pronounced for components manufactured for aerospace applications. For example, many aircraft parts made from titanium require 20 kgs of mill product for every 1 kg of finished product. In contrast, suitable powder metallurgy processes can produce the same product with

3 kgs of raw material for the finished component weighing 1 kg [4]. Also, because the powder metallurgical approach provides products having a fine grain structure, the machinability of parts made by P/M is superior to that made by I/M routes. Further, P/M approach can be used to make specialized products such as filters which can find extensive usage in chemical industry.

While P/M approach for titanium alloys till now has been exploited using (a) blended elemental (BE) powders or (b) prealloyed powders, there exists a third approach of using transient liquid phase sintering (TLPS) which also can be successfully exploited for manufacturing parts/preforms of titanium alloys. However, very little effort has been put towards the development of TLPS based processes. The present study was undertaken to study the transient liquid phase sintering behaviour of various binary, ternary and quaternary alpha and alpha-beta alloys of titanium. A limited number of tests were performed on hot isostatic pressing of prealloyed powders of Ti-6 Al-4 V. The present report discusses the results obtained in the present study. A broad literature review of powder metallurgy of titanium alloys has been presented first. Aims of the present investigation, experimental procedures and results obtained have been discussed subsequently.

CHAPTER - 2

POWDER METALLURGY OF TITANIUM ALLOYS - A REVIEW

2.1. Preparation of Powders of Titanium and its Alloys

Due to its very strong reactivity with most crucible materials, holding of liquid titanium for a reasonable period of time without its contamination poses serious problems. It is due to such reasons that powders of titanium and titanium alloys are not manufactured by conventional atomization methods. However, powders of titanium and its alloys can be produced by variety of other processes. These powders have been briefly described here while their relative advantages and disadvantages have been summarized in Table 2.1 [4].

2.1.1. Sponge Fine Production Process

Extraction of titanium consists of (a) beneficiation of titanium ore, (b) conversion of the enriched ore to titanium tetrachloride and (c) chemical reduction TiCl_4 using Mg or Na (Kroll's and Hunter's processes respectively). At this point, fines of unalloyed titanium sponge thus manufactured are screened out which can be used for P/M processes. Using this elemental powder for the production of powder metallurgy parts provides cheaper raw material since the subsequent processing and handling operations are eliminated. For the production of P/M titanium alloys, a master alloy is generally blended with the elemental titanium sponge powder which gets homogenized during sintering cycle. On the other hand, such a powder

TABLE 2.1. Relative advantages and disadvantages of various titanium powder production processes [4]

Powder Source (Price)	Description	Advantages	Disadvantages
Sponge (ESP)-Commercially-Pure and Elemental Master Alloy Blend (3-10 US \$ kg).	Obtained from Mg or Na-reduced titanium sponge fines. Leached to modify purity, flow or particle size. Irregular dendritic shape. U.S., U.K., Japan, U.S.S.R., manufacturers.	Least expensive source of powder. Large supply. Lowest energy required. Mechanical, hydraulic, or hydrostatic compaction.	Residual chloride fouls furnaces and causes porosity in welds. Welding is commercially acceptable if gas shielding is controlled.
Electrolytic-Commercially-Pure (10-14 US \$ kg).	Fused-salt electrolysis, using soluble anodes of sponge or scrap. Can also electrolyze $TiCl_4$. Requires 15 KWH per ton to make compared to 22 KWH Kroll process. U.S. and U.S.S.R. manufacturers.	High purity, modular equipment.	Pilot production facilities available only. New facilities will not be constructed until current sponge capacity exceeded.
Hydride-Dehydride (HDD)-Commercially-Pure and Elemental Blend Alloy (30-50 US \$ kg).	Uses the high solubility of H_2 to get a brittle hydride that is easily crushed. Powder is rough and equiaxed in appearance. Made from sponge, scrap, or ingot. U.S. manufacturer.	Possible vacuum dehydriding during sintering.	High-cost powder: limited-production powder.
Rotating Electrode Process (REP)-Commercially-Pure and Prealloy (20-60 US \$ kg).	Uses prealloy bar rotated at high speeds in an inert atmosphere while melted with an arc struck from a tungsten cathode. Small spherical droplets are spun off by centrifugal action. U.S. manufacturer.	Composition control high. High particle density. Best property results.	Tungsten inclusions that can cause fracture in some alloys. Ti-6Al-4V not affected. High-cost powder that must be hot isostatically pressed. HIP equipment capital investment is greater than \$1 million.
Centrifugal Shot Casting (CSC)-Commercially-Pure and Alloy (14-40 US \$ kg).	Uses an arc melting furnace with a stationary electrode and rotating water-cooled crucible. U.S. manufacturer.	Versatile feedstocks.	Also high cost.

contains small amounts of residual chlorides and other interstitials which can be detrimental to end properties of the product especially if it has to be used in high-performance applications and to be welded.

2.1.2. Rotating Electrode Process

As titanium sponge fines contain interstitial impurity atoms which can be eliminated only by melting under vacuum, such powders generally are not preferable for manufacturing heavy duty products. Also, titanium alloy powders cannot be manufactured by conventional atomizing processes. Atomized alloy powders of titanium alloys are therefore made by rotating electrode process (REP). In this method, a titanium alloy electrode is rotated at high speed and one end of the electrode is subjected to arc discharge in an inert gas or vacuum chamber. A tungsten electrode is generally used for the production of arc. Though satisfactory results can be obtained by this process, this process has the disadvantage that the titanium alloy powder produced is often contaminated with tungsten. Contamination of the powder, however, can be avoided by using a plasma arc instead of tungsten electrode. In such a case, the process is referred to as plasma rotating electrode process (PREP). Schematic diagram of this process is shown in Figure 2.1. Because of the spherical shape of particles produced by REP and PREP, these powders have poor compressibility. Hence hot deformation processes such as hot isostatic pressing (HIP) or hot pressing are required for the production of parts from these powders.

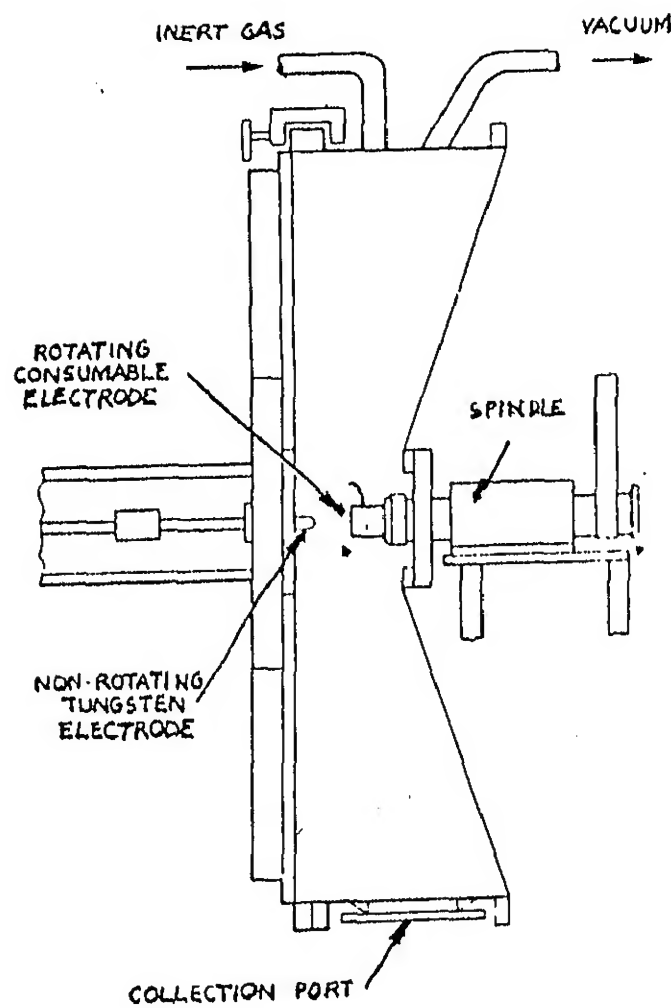


Figure 2.1. Schematic of REP apparatus [4].

2.1.3. Hydride-Dehydride Process

Another approach to make prealloyed titanium powders is that of hydride-dehydride formation. In such a process the alloy material, usually in the form of chips, is converted to a hydride by absorbing large amounts of hydrogen gas by reacting it with the material at high temperatures. Formation of hydride embrittles the material and it can be easily crushed or ground to a fine particle size. The powder is reheated slowly under vacuum and the hydrogen is pumped off due to the decomposition of the hydride.

2.1.4. Rapid Solidification Processes

Rapid solidification processes allow extended solid solubility, formation of metastable phases, structure refinement and freedom from segregation/workability problems [5,6]. A number of techniques are available which allows titanium to solidify rapidly [7]. The rapidly solidified product is often a powder, flakes or ribbons. Ribbons normally require further crushing. Several novel alloys of titanium are being synthesized by this approach. However, these processes are still in the exploratory stage.

2.2. Consolidation of Powders

Depending on the nature of powder used and the properties required for parts, various techniques have been followed for the consolidation of titanium and its alloy powders.

2.2.1. Consolidation of Elemental Powders

For the utilization of elemental powders, several consolidation choices have been used. These include cold pressing and sintering, isostatic pressing, slip casting, powder rolling, gravity sintering and forging.

2.2.1.1. Cold Pressing and Sintering

Cold pressing and sintering has been followed for the sintering of elemental titanium as well as titanium alloy powder premixes.

Abkowitz et al. [8] studied the sintering as well as forging of sintered preforms of commercially pure titanium powder. Sintered densities as high as 94% of theoretical density were obtained by cold pressing the powder at a pressure of 960 MPa followed by sintering at 1200°C. Pressed and sintered products, when forged to full density were found to have insignificant increase in strengths but were shown to have substantially higher ductilities. The powder processed commercially pure titanium products were reported to have better machinability compared to that obtained in wrought products. In the study of Lynch [9] consolidation of powder was done by conventional die compaction at pressures from 70 to 350 MPa and by isostatic pressing of compacts at pressures from 200 to 400 MPa. Sintering was done at 1100°C, 1300°C and 1500°C for a period 1 or 6 hours under vacuum. It was observed that repressing operation prior to sintering at 1300°C produced an increase in ductility in the as-pressed material. It was reported that the

improved mechanical properties were obtained by adopting such processing routes. Microstructural examination revealed the expected general correlation between decreased porosity and increased properties. Increasing the sintering temperature from 1100° to 1500°C caused progressive pore rounding and coarsening. Akechi and Hara [10] studied the behaviour of titanium powder compacts to understand the sintering kinetics during cyclic heating.

Sintering of cold pressed binary titanium alloys containing both α and β stabilizers have been studied by several authors. Adhesional reactions occurring during the sintering of refractory metals molybdenum, niobium and zirconium has been studied by Borisova and Kopichev [11] and Pavlov and Avrunina [12]. In the work of Pavlov and Avrunina premixes 1-9 wt % molybdenum, zirconium and niobium were pressed into blanks under a pressure of $5\text{-}7\text{ tons/cm}^2$ and were sintered. Similarly compaction and sintering behaviour of Ti-Ni shape memory alloys corresponding to the composition TiNi were studied by Igharo and Wood [13]. Sponge titanium powder and carbonyl nickel powder were blended and pressed at pressures ranging from 155-929 MPa by die compaction and 171-503 MPa by isostatic pressing. Sintering was done under a vacuum of 10^{-9} MPa for 1 hr at temperatures $600\text{-}1000^{\circ}\text{C}$. The presence of diffusional porosities in regions of nickel particle in the sintered compacts showed that nickel diffused faster than titanium.

Cold pressing and sintering has also been followed for multicomponent titanium alloy systems such as Ti-6 Al-4 V [14-18]. For the studies on this and similar alloys sponge titanium

and Al-V master alloy taken as the starting material. Powder premixes were cold pressed under 400 MPa pressure and then sintered at about 1300°C under vacuum. Characterisation of fracture surface, pores and inclusions of sintered Ti-6 Al-4 V was done by Welsch et al. [17]. Ti-10 V-2 Fe-3 Al was also studied by cold pressing and sintering route by Boyer et al. [19].

2.2.1.2. Slip Casting/Gravity Moulding

Many of the applications for titanium involve components having a high surface area such as electrodes and filters to be used in corrosive environments. In such cases methods for processing studied include gravity moulding and slip casting. The permeability and pore size are controlled by careful selection of powder particle size and shape and the parts are sintered under closely controlled conditions. Titanium porous bodies ranging from 25% to 75% theoretical density have been manufactured by Gould Inc., U.S.A. [4].

2.2.1.3. Forging/Rolling/Extrusion

The incorporation of forging/rolling/extrusion in conjunction with the as-sintered powder metallurgy forms yields products which have comparable properties with their equivalent wrought products.

Forging preforms offer inexpensive forging stock and production of a more equiaxed, fatigue-resistant microstructure [20-24].

Pressed and sintered products with an initial density of 94% of theoretical, when forged to full density were found

to have shown substantially higher ductilities [8]. Post-sinter densification of cold-pressed and sintered Ti-6 Al-4 V was carried out using a soft tooling by Ceracon process utilizing a granular pressing medium around the sintered compact and conventional hot forging [25]. Weiss et al. [18] studied the effect of isothermal forging on microstructure and fatigue behaviour of Ti-6 Al-4 V sintered compacts.

Powder metallurgy component production generally involves powder production and consolidation as separate steps [5]. However, cost reduction is possible by converting the powder directly into a mill product [26-32]. This has been done using the blended elemental approach to produce foil, sheet and plate [28,29]. The plate was produced by rolling a compacted billet, the foil and sheet were fabricated directly from the powder as shown schematically in Figure 2.2.

2.2.2. Consolidation of Prealloyed Powders

Because of the compacting difficulties associated with the spherical REP and PREP powders, hot deformation processes such as hot isostatic pressing are followed. Direct processing methods such as extrusion are also followed for the prealloyed powder.

2.2.2.1. Hot Isostatic Pressing (HIP)

Extensive studies on prealloyed Ti-6 Al-4 V powder metallurgy parts have been carried out [5,35,36]. Engine mount supports for F-18 aircraft were made from prealloyed powder by HIPing with ceramic mould process [36] and these parts were

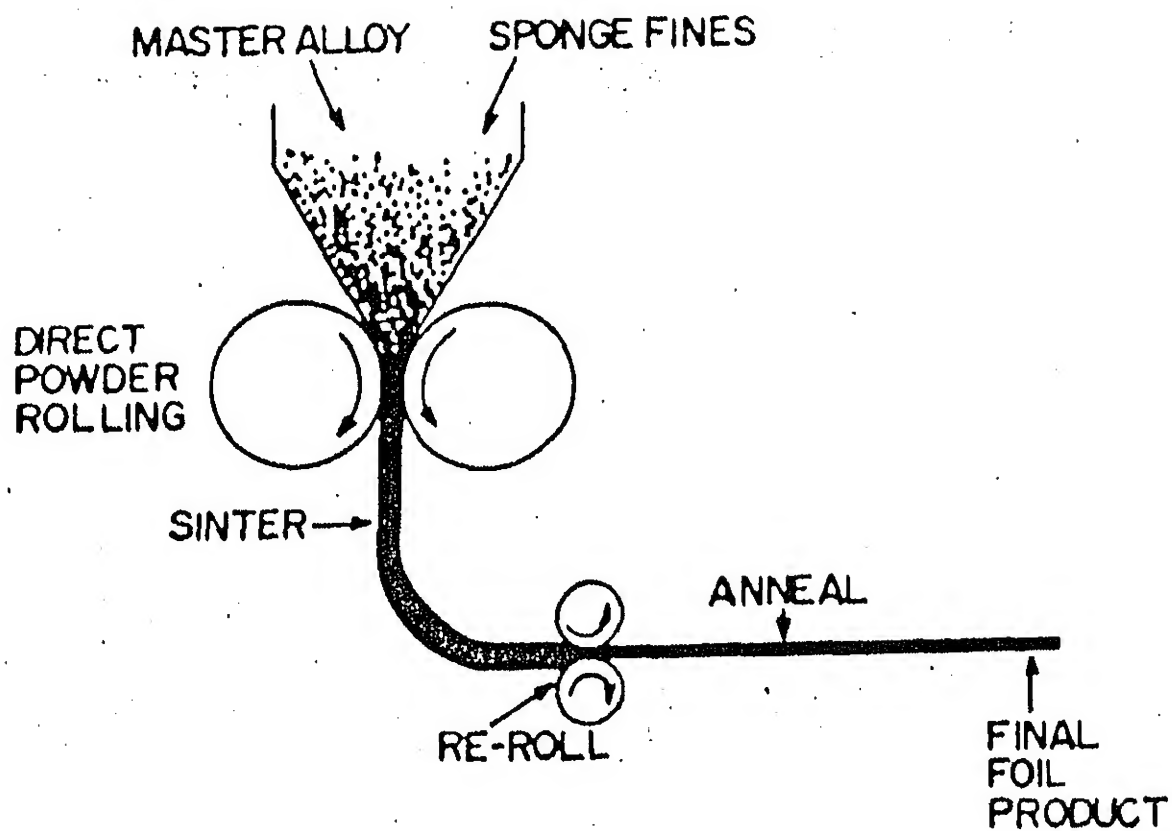


Figure 2.2. Schematic diagram showing the fabrication of compacted titanium powder directly to a sheet.

found to have properties equivalent to those of wrought material used for the same parts. Fluid die compaction was followed for prealloyed Ti-6 Al-4 V powder [25]. Work on prealloyed Ti-10 V-2 Fe-3 Al and Ti-6 Al-4 V powders demonstrated that at higher pressures full compaction and bonding can be accomplished at temperatures as low as 650°C [37]. The low compaction temperatures developed a very fine microstructure which exhibits excellent combinations of tensile strength and elongation for Ti-6 Al-4 V alloy. The aspect ratio of α -plates can be decreased by HIP'ing and it is found that fatigue initiation resistance at room and elevated temperatures can be improved with small equiaxed α -morphology [38-40]. It was found that the alpha aspect ratio can be decreased by deforming the powder before compaction using the strain energising process [41,42].

2.2.2.2. Rolling/Forging/Extrusion

The microstructure of prealloyed Ti-6 Al-4 V compacts were modified by thermomechanical processing [43]. It was found that $\alpha + \beta$ forging of the powder compacts followed by an $\alpha + \beta$ solution treatment improved the low cycle fatigue strength of Ti-6 Al-4 V significantly [44].

Direct processing to mill products was followed for the prealloyed titanium powders. It was reported that titanium powders can be consolidated by extrusion in an evacuated can. In the case of Ti-6 Al-6 V-2 Sn, tensile and fracture properties equivalent to wrought levels were obtained [4].

2.2.3. Consolidation of Rapidly Solidified Powders

The most comprehensive study done on rapidly solidified conventional titanium alloys has been on Ti-6 Al-4 V alloy [45]. Some work on Ti-Mo-Al $\alpha + \beta$ alloy was done by Belov and Polkin [46].

2.3. Transient Liquid Phase Sintering (TLPS)

Not much literature is available regarding the TLPS of titanium alloys. The effect of compact growth during the TLPS of Ti-Al alloys has been studied by several authors [47,48]. Results of Savitskii [47] showed that lattice growth takes place due to alloying brought about by diffusion or due to the formation of intermetallic compound. It was found that the formation of intermetallic compounds is highly exothermic and sintering can be carried out at relatively low temperatures. Yixiang et al. [48] studied the void formation effect of interdiffusion between titanium and aluminium metal powders. Nakamura and Kaieda [49] studied the microstructure and mechanical properties of sintered TiAl. Powder metallurgy of titanium aluminides was reported by Moxson and Friedman [50].

TLPS study on titanium containing tin and aluminium was done by Khromov [51] by carrying out dilatometric studies to produce porous titanium alloys. It was found that Ti-6 Al compacts showed initial compact growth and subsequent shrinkage.

CHAPTER - 3

AIMS OF THE PRESENT INVESTIGATION

The present investigation is concerned with the study of Transient Liquid Phase Sintering (TLPS) behaviour of multi-component titanium alloys. Two categories of titanium alloy compositions corresponding to α and $(\alpha + \beta)$ alloys, have been selected and their sintering behaviour in the presence of transient melts of Al, Sn and/or Al-Sn has been studied. The aims of the present investigation are

- (1) Characterization of the effect of liquid content on the sintering behaviour of binary and ternary α alloys in the Ti-Al-Sn system.
- (2) Characterization of the effect of liquid content on the sintering behaviour of quaternary $(\alpha + \beta)$ alloys of titanium in the Ti-Al-V-Sn system.
- (3) Studying the homogenizing behaviour of quaternary Ti-Al-V-Sn alloys obtained by their transient liquid phase sintering.

The volume content of the liquid has been changed by varying the amount of Al, Sn or both in the premixes. Sintering behaviour of the multicomponent alloys has been studied in terms of sintered density, amount and nature of the porosity present, homogeneity of the chemical composition, microstructure and hardness. A few experiments have been performed on hot isostatic pressing of prealloyed Ti-6 Al-4 V powder and effect of different heat treatments on the microstructure and properties of HIPped material has been reported.

CHAPTER - 4

EXPERIMENTAL PROCEDURE

Titanium powder supplied by SPMS-Powder Met., France, aluminium powder supplied by Valimet Inc., U.S.A., tin powder supplied by Kochlite, U.K., V-Al master alloy supplied by Union Carbide Corporation, U.S.A. and prealloyed Ti-6 Al-4 V powder supplied by Nuclear Metals Inc., U.S.A. were used as base materials.

4.1. Powder Characteristics

Relevant details of the powders used were given below in Tables 4.1-4.5.

TABLE 4.1. Characteristics of Titanium Powder

Purity	99.5%
Shape	Irregular
Type	Sponge
Particle size	13 μm (FSSS)
Apparent density	1.3 g/cc
Flow rate	Non free flowing

TABLE 4.2. Characteristics of Aluminium Powder

Shape	Spherical
Type	Atomized
Particle size	5.1 μm (FSSS)
Apparent density	0.86 g/cc
Flow rate	Non free flowing

TABLE 4.3. Characteristics of Tin Powder

Shape	Rounded
Type	Atomized
Particle size	2.7 μm (FSSS)
Apparent density	1.63 g/cc
Flow rate	Non free flowing

TABLE 4.4. Characteristics of V-Al Master Alloy Powder

Shape	Irregular
Particle size	9.4 μm (FSSS)
Apparent density	1.45 g/cc
Flow rate	Non free flowing
Composition	Wt %
Vanadium	61.03
Aluminium	38.661
Boron	0.001
Carbon	0.008
Molybdenum	0.04
Silicon	0.21
Oxygen	0.05

TABLE 4.5. Characteristics of Prealloyed Ti-6 Al-4 V Powder

Shape	Spherical
Type	REP
Apparent density	2.64 g/cc
Flow rate	28 s/50 g
Particle size, μm	wt %
500	0.01
354	3.62
250	7.37
177	26.78
125	50.15
88	10.07
63	1.89
44	0.11
<40	0.01
Composition	wt %
C	0.017
Al	6.46
V	4.05
Fe	0.19
O ₂	0.19
N ₂	0.007
H ₂	0.0019
Y	<0.001

4.2. Particle Size Analysis of Powders

The particle size distributions of the sponge fine titanium, aluminium, tin and V-Al master alloy powders were determined using Coulter Counter Model Z_B and B. This method is based on measuring the change in electrical resistance when particles suspended in electrical conducting liquid pass one by one through an aperture in between the electrodes. The change in resistance produces voltage flux which is proportional to the particle volume. Particle size determined by this method is defined by the cube root of particle volume. Trisodium phosphate and $KClO_4$ were used respectively for titanium and V-Al master alloy powders whereas NaCl was used for aluminium and tin powders. The particle size distribution of the powders as obtained from Coulter Counter analysis were presented in Figure 4.1.

4.3. Powder Morphology

Morphology of powders, an important variable in TLPS, was ascertained by viewing powder particles under JEOL JSM 840A scanning electron microscope (SEM) under an operating voltage of 20 kV. While titanium powder was found to have a typical sponge morphology having intricate intra-particle pore channels, V-Al master alloy powder has irregular shape with intra-particle pore channels. Aluminium and tin powder particles had a nearly spherical shape with negligible intra-particle porosity. Typical micrographs of these powders are shown in Figure 4.2.

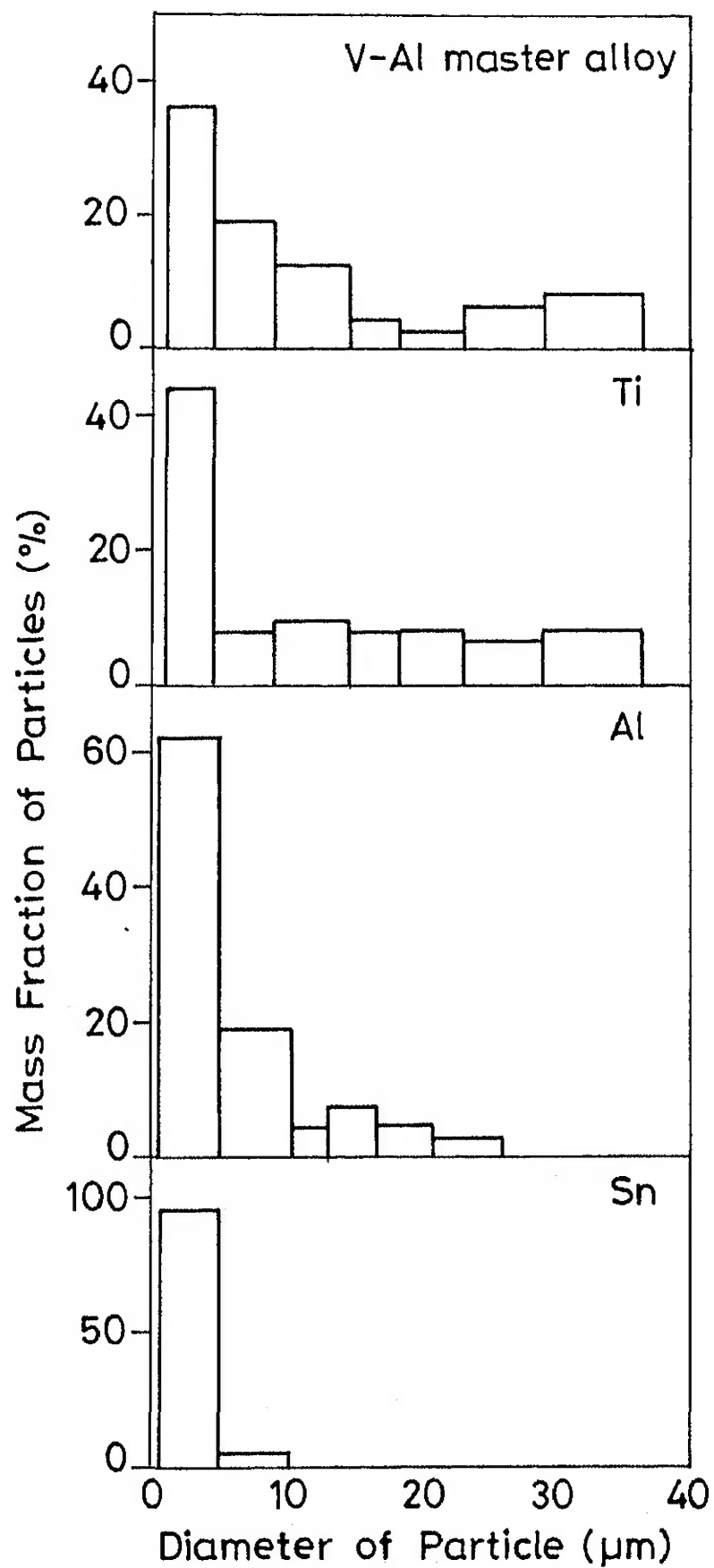
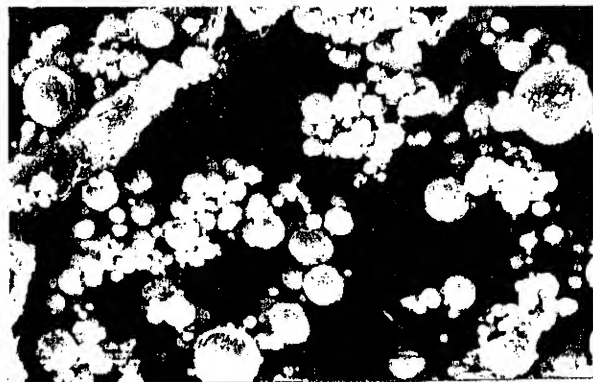


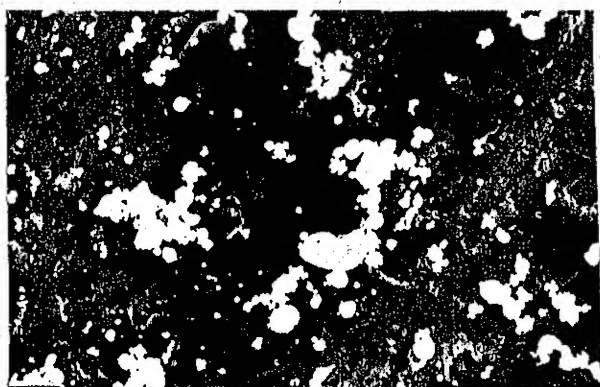
Fig.4.1 Particle size distribution of different powders from Coulter Counter analysis.



(a)



(b)



(c)



(d)

Figure 4.2. SEM photomicrographs of various powders (a) Ti, (b) Al, (c) Sn and (d) V-Al master alloy showing aggregate of powder particles. 1000X

4.4. Premix Preparation

Powder premixes corresponding to the chemical compositions of Ti-1 Sn, Ti-2 Sn, Ti-5 Al, Ti-5 Al-2.5 Sn, Ti-5 Al-5 Sn and Ti-6 Al-6 V-xSn ($x = 0, 1, 2, 3$) (all compositions in wt %) were taken. Blending was done mechanically using a mortar and pestle for 3.6 ks (1 hr).

4.5. Green Compaction

Titanium powder and premixes corresponding to the compositions studied were compacted into cylindrical pellets in a steel die using a 20 T capacity hydraulic press under a pressure of 380 MPa. The compacts were of 12.7 mm diameter and 7-8 mm in height. The die wall was lubricated with zinc stearate prior to powder filling. Height and diameter of the pellets were measured using a Vernier calipers and from these, the volumes of the pellets were determined. Their weights were determined using a single pan automatic balance. From the weights and volumes, their densities were calculated. In all the cases, the green compacts were found to have 64-66% of the theoretical density.

4.6. Sintering

A resistance type vacuum tubular furnace having silicon carbide heating elements was used for sintering. The furnace tube was made of alumina which had a constant temperature zone of 45 mm at 1300°C. Temperature of the furnace was measured by a platinum/platinum - 10% rhodium thermocouple. An on-off controller was used for temperature control.

Green compacts were sintered in a vacuum corresponding to lesser than 10^{-2} m bar at 1300°C (1573 K) for 1 hr (3.6 ks). Green compacts of Ti-6 Al-6 V-xSn were sintered at 1200°C (1473 K) also. After the sintering period was over, samples were vacuum cooled at the rate of 0.03 c/s upto 100°C (373 K) and were subsequently air cooled to room temperature.

Few samples corresponding to the compositions of Ti-5 Al and Ti-5 Al-5 Sn were sintered under argon atmosphere at 660°C (933 K) for 15 min (0.9 ks) and were water quenched subsequently.

4.7. Hot Isostatic Pressing

The Ti-6 Al-4 V prealloyed powder was canned in 12 mm diameter mild steel tube, which was sealed under vacuum. HIP'ing of the canned prealloyed Ti-6 Al-4 V was performed on ASEA HIP unit at Defense Metallurgical Research Laboratories, Hyderabad. HIP'ing was done under an argon atmosphere and the cycle consisted of holding the canned powder at 1160°C (1433 K) at a pressure of 1.215 K bar (121.5 MPa) for 3 hr (10.8 ks). The HIP'ed tube was subsequently mechanically stripped off and Ti-6 Al-4 V rods of 100 mm length were obtained.

4.8. Heat Treatment

Homogenizing treatments were given to sintered Ti-6 Al-6 V-xSn alloys as it was found that microstructural inhomogeneities existed in the as-sintered alloys. Since the as-sintered α titanium alloys of Ti-Sn, Ti-Al and Ti-Al-Sn alloys were confirmed to have uniformity in microstructure and alloying element distribution, they were not subjected to any further

treatment. HIP'ed Ti-6 Al-4 V were given two different heat treatments.

4.8.1. Homogenizing of Ti-6 Al-6 V-xSn Alloys

Two different temperatures were selected for homogenizing: (i) in the α -phase at 850°C (1123 K) for 5 hr (18.0 ks) and (ii) in the β -phase at 1000°C (1373 K) for (a) 4 hr (14.4 ks) and (b) 20 hr (7.2 ks).

Homogenizing was done in the same furnace used for sintering. Vacuum corresponding to lesser than 10^{-2} m bar was used. After homogenizing samples were furnace cooled under vacuum to room temperature at a rate of 0.03°C/s.

4.8.2. Solution Treating/Overaging (STOA) and Mill Annealing of HIP'ed Ti-6 Al-4 V

4.8.2.1. STOA Treatment

For this treatment, the HIP'ed alloy was solution treated at 1055°C (1328 K) for 2 hr (7.2 ks) in air and then water quenched. The water quenched alloy was given an ageing treatment at 705°C (978 K) for 2 hr (7.2 ks) and then air cooled to room temperature.

4.8.2.2. Mill Annealing

For mill annealing, the HIP'ed alloy was heated at 705°C (978 K) for 2 hr (7.2 ks) and then air cooled to room temperature.

4.9. Evaluation of Sintered Properties

The following properties of the compacts were measured after sintering.

4.9.1. Density and Porosity Measurements

Sintered densities of the pellets were measured by the displacement method using xylene as the impregnating liquid. The sintered density, interconnected and closed porosities were measured by the following formulae as suggested by Arthur [52]

$$\text{Sintered density} = \frac{A}{B - C} \text{ g/cc}$$

where

A = Weight of the sintered compact in air, g

B = Weight of the xylene impregnated sintered compact in air, g

C = Weight of the xylene impregnated sintered compact in water.

Sintered density was expressed as a percentage of the theoretical density. The theoretical densities of the compacts were calculated by the rule of mixture where literature data is not available.

$$\text{Interconnected porosity} = \frac{B - A}{B - C} \times 100$$

$$\text{Closed porosity} = \text{Total porosity} - \text{Interconnected porosity}$$

Total porosity was measured as explained in Section 4.9.2.

4.9.2. Determination of Total Porosity and Pore Size Distribution

Total porosity was measured by quantitative metallography by measuring the volume fraction of the pores in the compact using image analysis. Samples for porosity measurement under image analyser were prepared following the normal procedure used for microstructural observation as explained in 4.10.1. Samples were observed under an optical microscope which was attached with an image analyser (OMNICON alpha 500 Bausch & Lomb make).

Porosity distribution was obtained by measuring the number of pores greater than a certain size using the oversize count of the image analyser. Measurements were done at 15 different fields for each sample and the average value was taken.

4.9.3. Hardness Measurements

4.9.3.1. Macrohardness

Vickers hardness measurement of the sintered compacts was measured on Model HPO 250 of 'FHL' make Hardness Testing machine using a load of 5 kg. Three indentations were taken on each polished specimen and the average value was reported.

4.9.3.2. Microhardness

Microhardness measurements were done on titanium, Ti-1 Sn, Ti-2 Sn, Ti-5 Al, Ti-5 Al-2.5 Sn and Ti-5 Al-5 Sn samples using Leitz Miniload Microhardness Tester to find out the variation of alloy hardening within a grain to understand the alloying distribution inside a grain. Three indentations

were made in each grain of the polished and etched specimens.

4.10. Microstructural Examination

4.10.1. Optical Microscopy

Samples for observation under the optical microscope were prepared by the normal procedure. The surface of the sample was ground flat using a belt surfacer. This sample was polished successively on 1/0 through 4/0 emery paper taking care that no scratches are produced during polishing. The specimens were thoroughly washed in water and wheel polished using a 5 μ m alumina suspension. Final polishing was done on a relatively low speed wheel rotated at 250 rpm. A solution consisting of 20 ml HF, 20 ml HNO₃ and 40 ml glycerol was used as the etching agent for Ti and Ti-Sn, Ti-Al and Ti-Al-Sn alloys. For Ti-6 Al-6 V-xSn alloys, a solution of 10 ml HF, 5 ml HNO₃ and 85 ml H₂O was used as the etching agent.

Samples were observed under Leitz Metallux 3 Optical microscope in the unetched and etched conditions.

4.10.2. Scanning Electron Microscopy

Morphology of the powders used in the present study was observed under JEOL JSM 840A Scanning Electron Microscope (SEM) using an operating voltage of 20 kV in the secondary electron mode. Samples in the polished and etched conditions were also observed under SEM.

Some of the samples from Ti-Al, Ti-Al-Sn system and as-sintered and homogenized Ti-6 Al-6 V-xSn alloys were observed under SEM and were subjected to elemental analysis by energy

dispersive system EDAX. Samples for microstructural observation under SEM were prepared by the same procedure followed for optical microscopy.

4.11. Fractography

Since the understanding of the response of material during its mechanical loading can be assisted by examining samples fractured during tensile tests, fractography of as-HIP'ed and heat treated Ti-6 Al-4 V was done in the present work. Fractured samples were examined under JEOL JSM 840A scanning electron microscope in the secondary electron mode under an operating voltage of 15 kV.

CHAPTER - 5

RESULTS

As mentioned earlier since very little work has been done in the field of transient liquid phase sintering of titanium alloys, in the present study, transient liquid phase sintering of some α and $\alpha + \beta$ titanium alloys has been studied. Results obtained during this study have been presented in this chapter.

5.1. Transient Liquid Phase Sintered α -Titanium Alloys

The results obtained from the studies of TLPS of Ti-1 Sn, Ti-2 Sn, Ti-5 Al, Ti-5 Al-2.5 Sn and Ti-5 Al-5 Sn alloys were presented below.

5.1.1. Densification

Sintered density of pure titanium and different binary and ternary alloys sintered at 1300°C (1573 K) for 1 hr (3.6 ks) has been shown in Figure 5.1. It can be seen that the sintered density of titanium improves, in general, with alloying additions. Assuming that the total aluminium and tin contents added in pre-mixes form a liquid phase in proportion to their weight percentages, the volume content of the liquid phase present at the beginning of TLPS was estimated. Sintered density of various alloys as a function of amount of liquid formed has been shown in Figure 5.2. These results show that the rate of increase in density with respect to volume fraction of liquid phase was higher for Ti-Sn alloys than Ti-Al alloys. Similarly, the slope

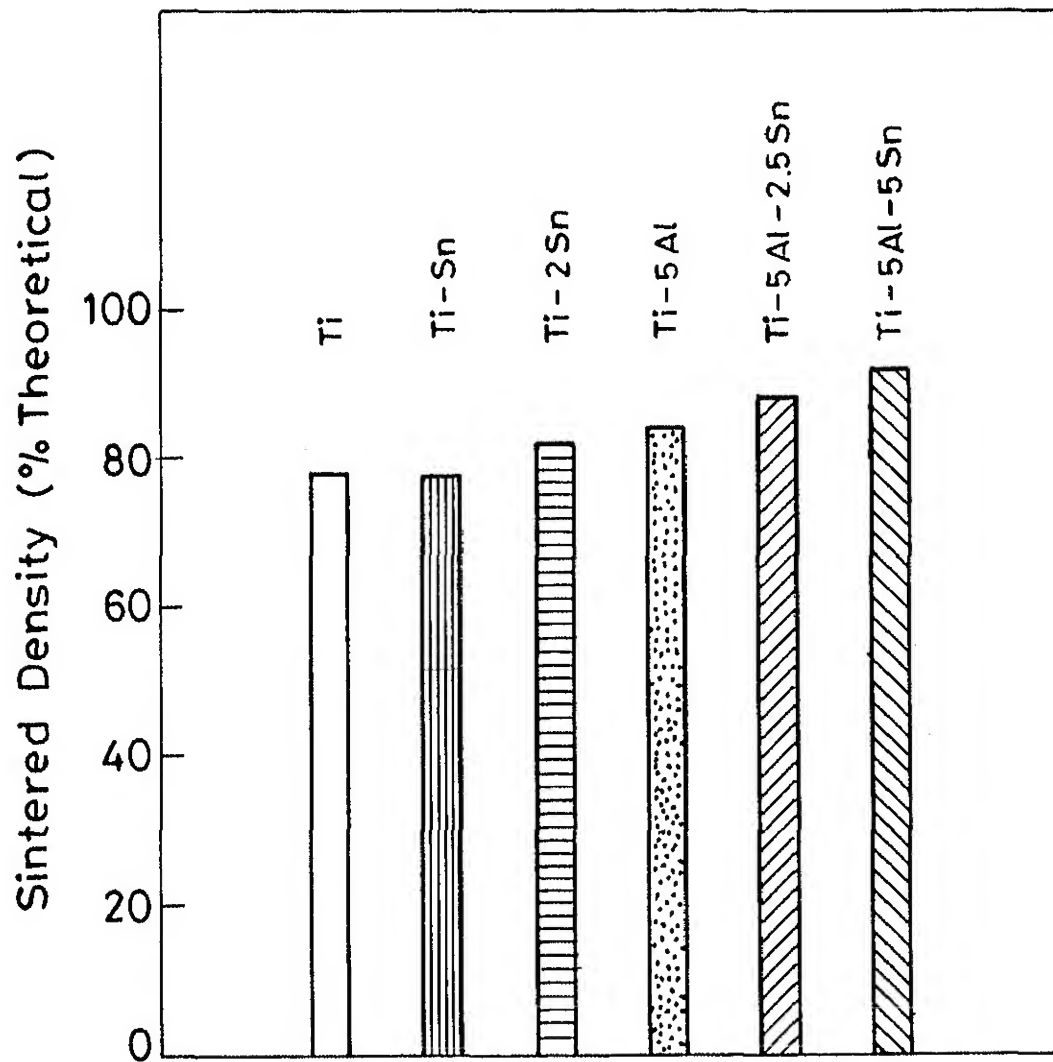


Fig.5.1 Sintered density variation of various alloys.

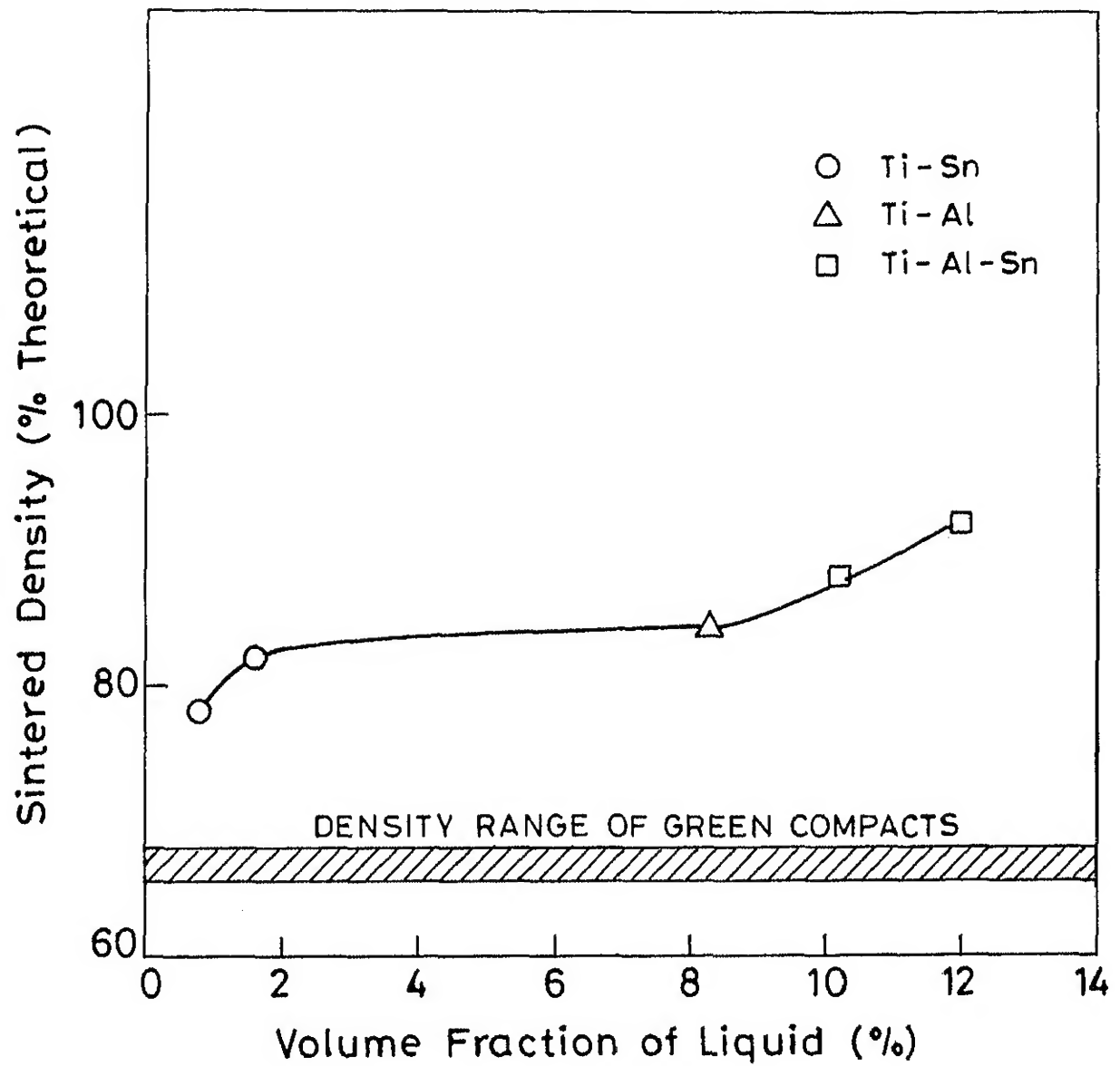


Fig.5.2 Variation of sintered density of Ti-base alloys with liquid volume fraction.

of the curve increased in ternary Ti-Al-Sn alloys with increasing amount of tin in the alloy.

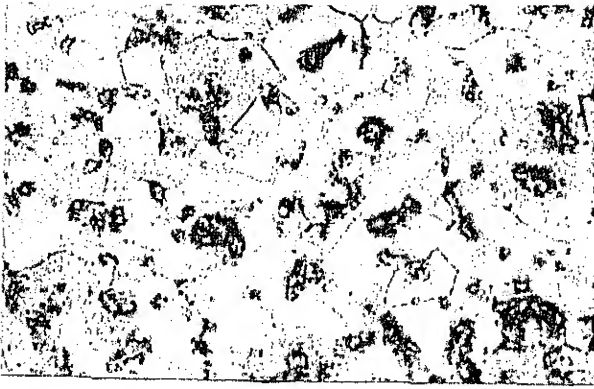
5.1.2. Microstructure and Pore Characteristics

Microstructures of the as-sintered alloys have been shown in Figure 5.3. In all the cases, the alloys consisted of equiaxed grains of α -phase. Grain sizes of different sintered alloys, measured by the Jefferies' line count method [53] have been shown in Table 5.1. These results show that while the addition of tin in both binary and ternary alloys decreased the grain size, the addition of aluminium exhibited an opposite trend.

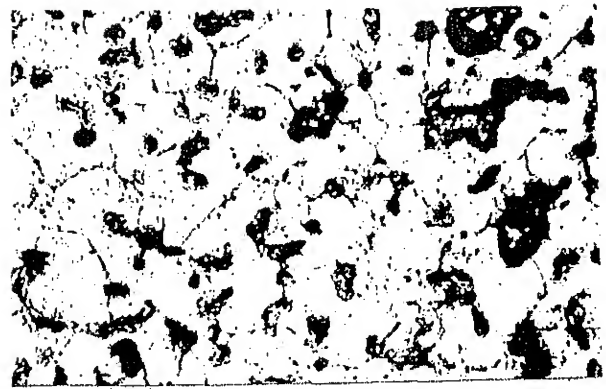
The examination of etched microstructures of different as-sintered alloys also revealed that most of the pores were found to be lying at grain boundaries or triple points. Existence of a few intra-particle pores can possibly be explained due to the spongy characteristics of the starting titanium powder used.

Size distribution of pores present in different alloys were obtained by examining their microstructures in the unetched condition shown in Figure 5.4. Results obtained have been shown in Figure 5.5. It is clear from these histograms that the pore size distribution in all the investigated alloys was positively skewed with most of the pores being in the size range of 0-20 μm .

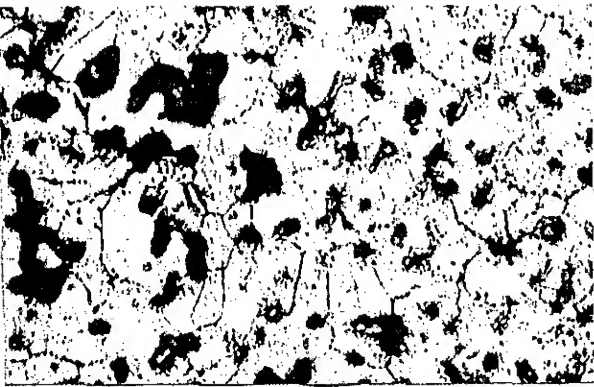
Volume fractions of interconnected and closed porosities in various sintered alloys has been shown in Figure 5.6. It can be seen that the volume fraction of the closed porosity decreased with the addition of tin in binary Ti-Sn as well as ternary



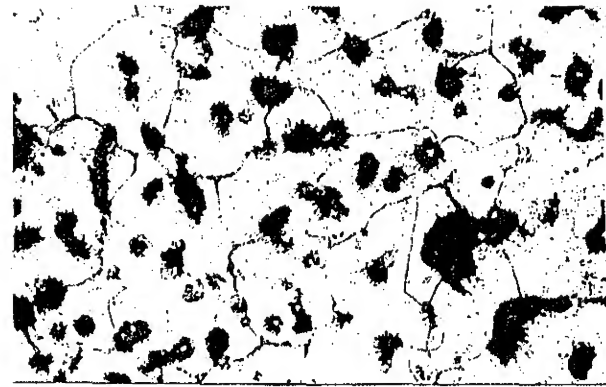
(a)



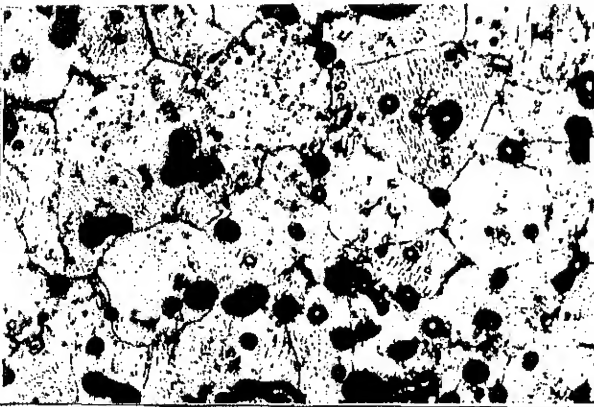
(b)



(c)



(d)



(e)

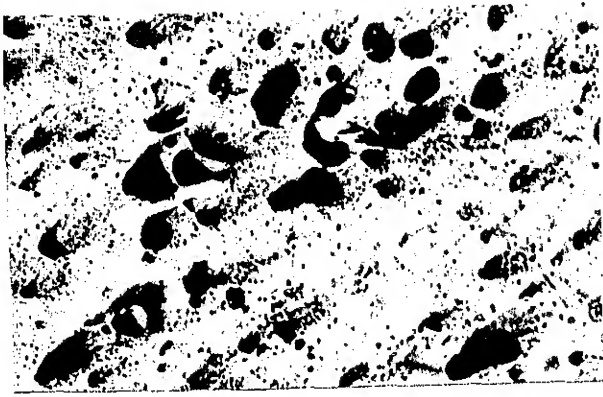


(f)

Figure 5.3. Optical micrographs of various sintered titanium alloys (a) Ti, (b) Ti-1 Sn, (c) Ti-2 Sn, (d) Ti-5 Al, (e) Ti-5 Al-2.5 Sn and (f) Ti-5 Al-5 Sn. 200X

TABLE 5.1. Grain Size Variation of Various Sintered Ti-alloys

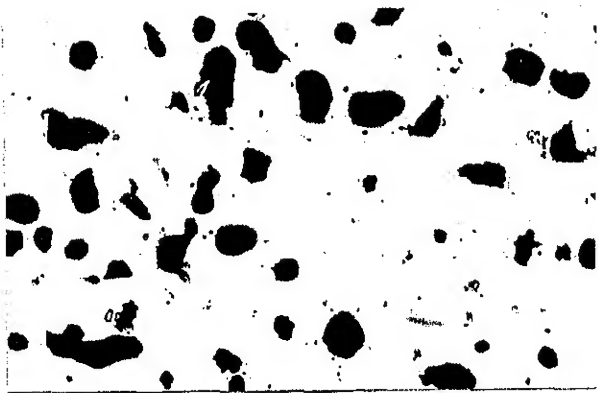
Alloy	Grain size (μm)
Ti	44.9
Ti-1 Sn	44.3
Ti-2 Sn	39.9
Ti-5 Al	58.5
Ti-5 Al-2.5 Sn	58.9
Ti-5 Al-5 Sn	47.2



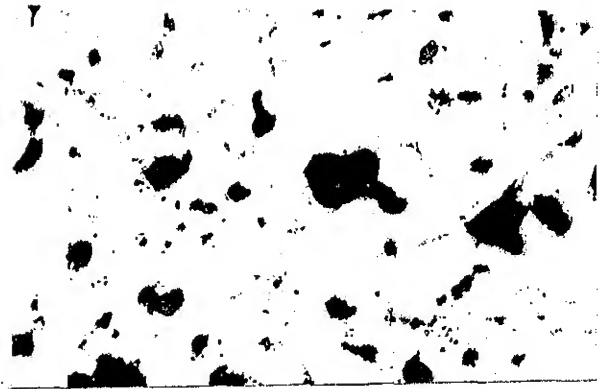
(a)



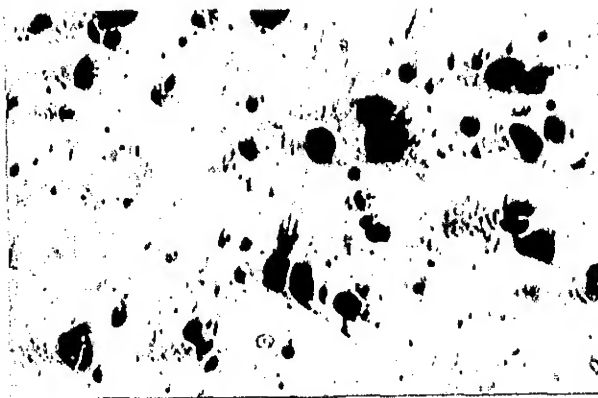
(b)



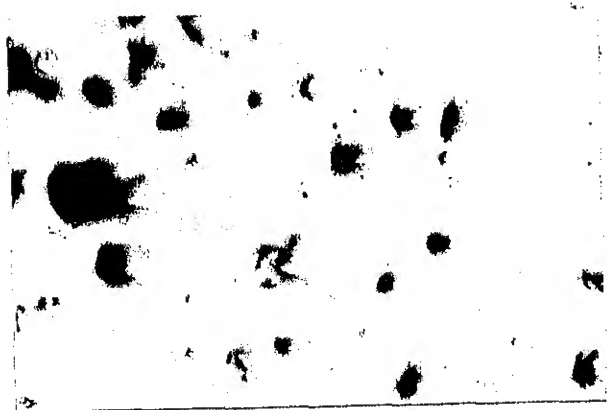
(c)



(d)



(e)



(f)

Figure 5.4. Optical micrographs of various sintered Ti-base alloys showing pores and their distributions (a) Ti, (b) Ti-1 Sn, (c) Ti-2 Sn, (d) Ti-5 Al, (e) Ti-5 Al-2.5 Sn and (f) Ti-5 Al-5 Sn. 200X

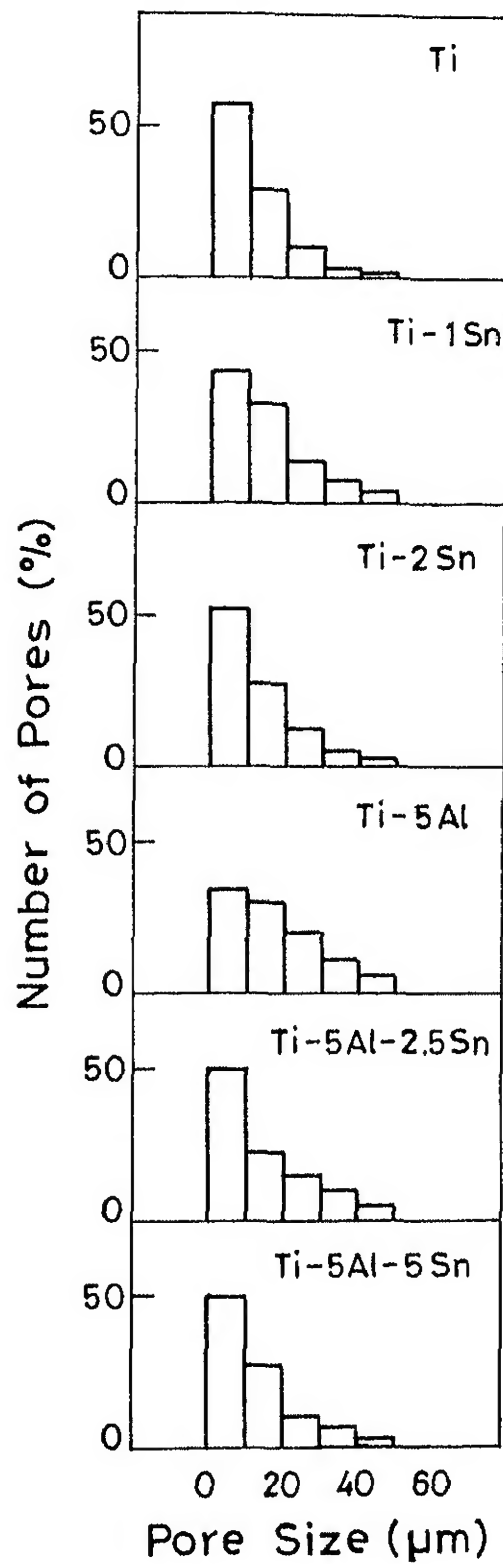


Fig.5.5 Pore size distribution of different sintered titanium alloys from image analysis .

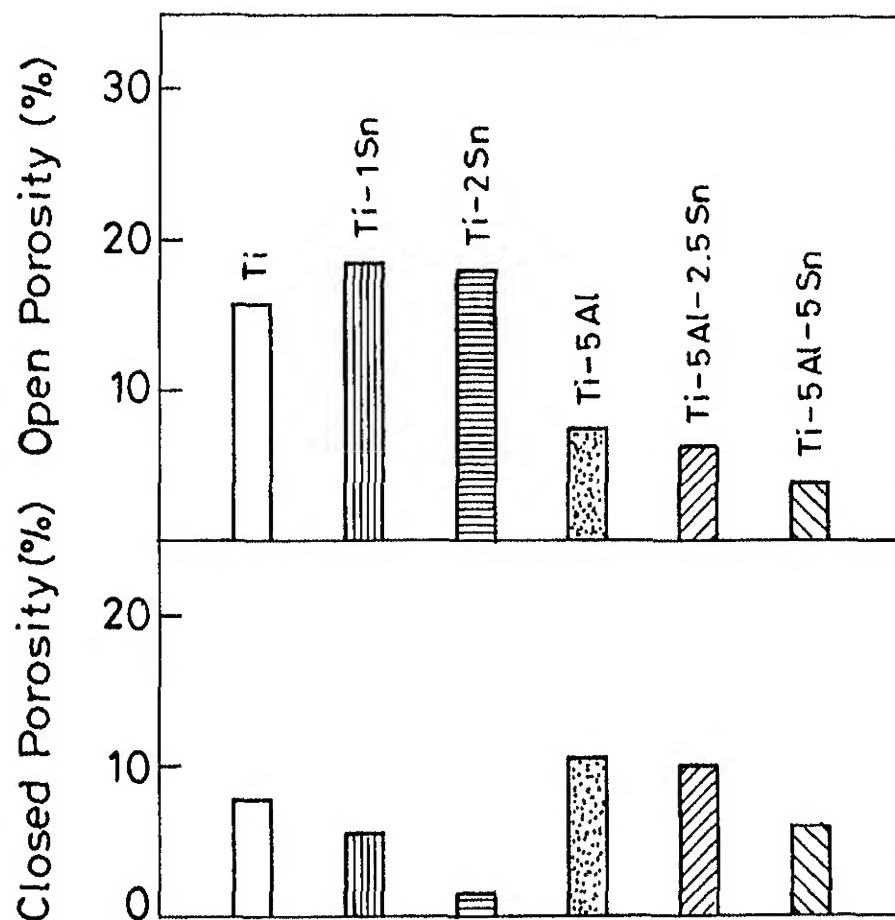


Fig.5.6 Effect of different alloying elements on the nature of porosity of sintered titanium.

Ti-Al-Sn alloys. The addition of aluminium in titanium, on the other hand, increased the volume fraction of closed porosity.

Optical and scanning electron micrographs of Ti-5 Al and Ti-5 Al-5 Sn alloys sintered under argon atmosphere at 660°C (933 K) for 15 min (0.9 ks) and subsequently water quenched have been shown in Figure 5.7. Results obtained from EDAX of these samples observed under SEM have been shown in Table 5.2. It is clear from these results that formation of intermetallics such as Ti_3Al occurs at few places during the progress of sintering of these alloys.

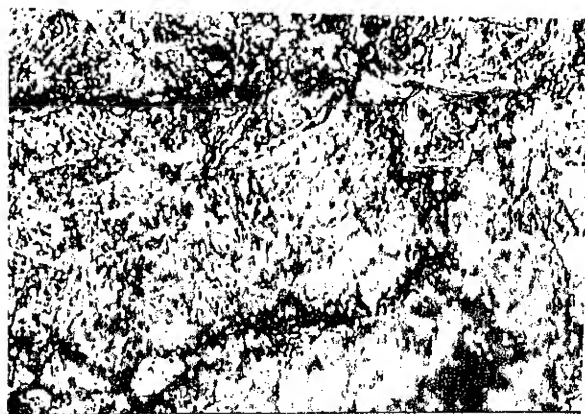
5.1.3. Hardness of Alloys

Macrohardness values of various sintered alloys have been shown in Figure 5.8. It is clear from these results that the sintered hardness of titanium increased with alloying additions. Aluminium, however, found to be more effective hardener when compared to tin.

In order to examine the homogeneity of alloying additions in various sintered compacts, microhardness measurements within different grains were made on polished and etched microstructures. These measurements indicated that the structure consisted of fairly uniform distribution of alloying additions. Representative plots between microhardness and the distance from grain/particle boundary have been shown in Figure 5.9. These microhardness variations indicate more or less uniform distribution of alloying additions with slight tendency for their segregation at grain/particle boundaries. These findings were subsequently confirmed by EDAX results also.



(a)

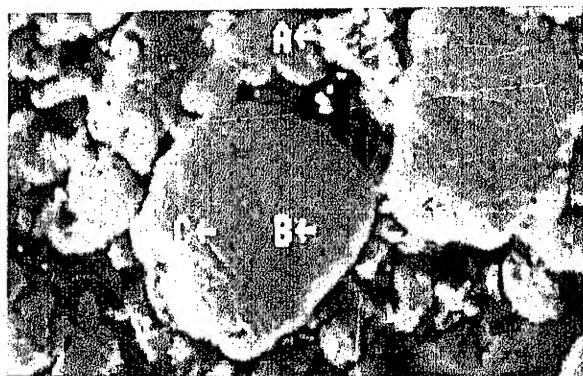


(b)

1000X



(c)



(d)

Figure 5.7 (a,b) Optical and (c,d) scanning electron micrographs of Ti-5 Al and Ti-5 Al-5 Sn alloys respectively sintered at 660°C for 15 min and subsequently water quenched.

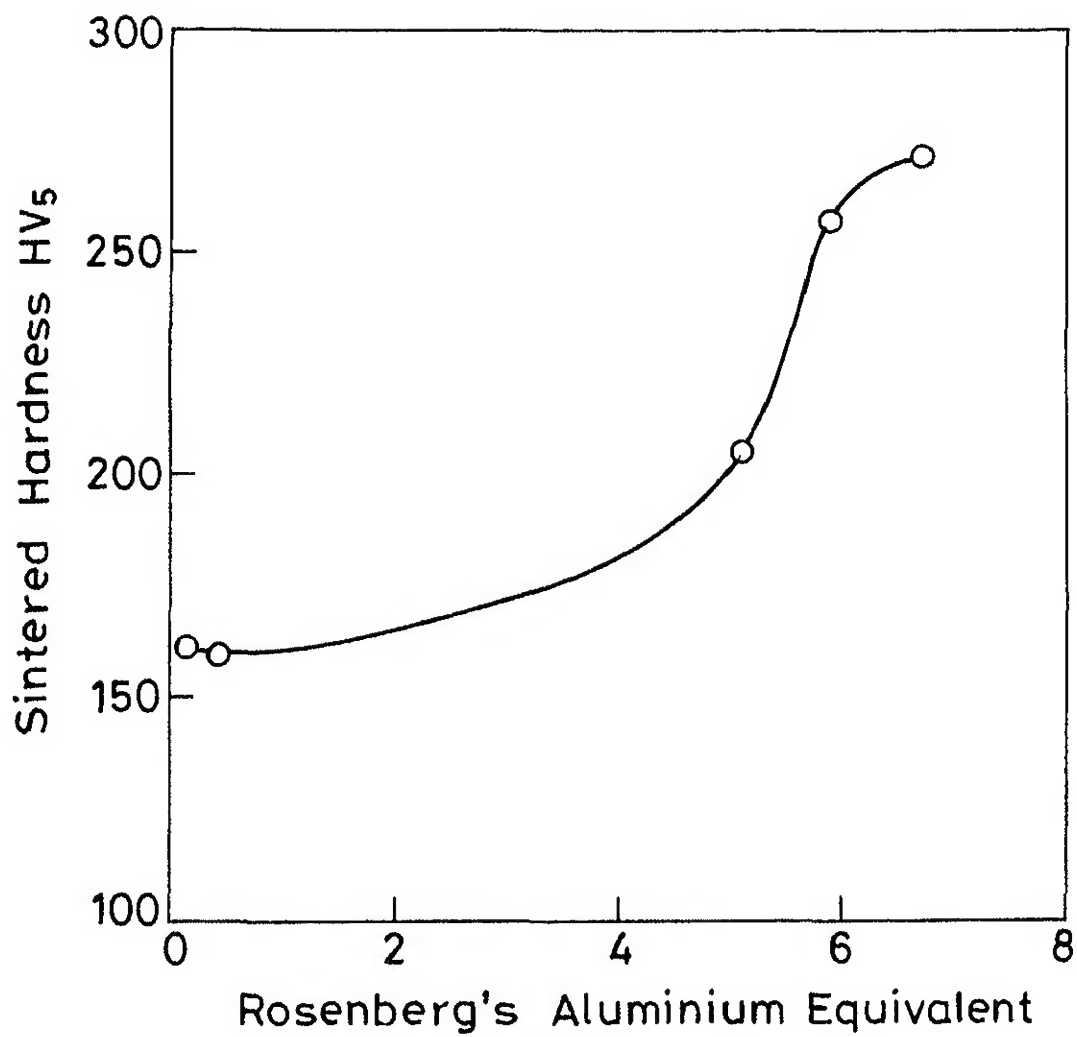


Fig.5.8 Variation of sintered hardness with Rosenberg's aluminium equivalent.

TABLE 5.2. Typical EDAX analysis of Ti-5 Al and Ti-5 Al-5 Sn premix route alloys sintered at 933 K for 900 s and subsequently water quenched

Alloy	Location in the micro-structure	Variation of alloying elements (wt %)		
		Ti	Al	Sn
Ti-5 Al (Figure 5.7.a)	A	96.50-100	10-3.50	-
	B	100	0	-
	C	86.3 -100	0-13.7	-
Ti-5 Al-2.5 Sn (Figure 5.7.b)	A	94.80-96.6	0.02-0.29	3.12-5.22
	B	93.44-97.24	0-0.11	2.71-2.76
	C	69.66-81.90	1.80-12.49	16.30-17.85

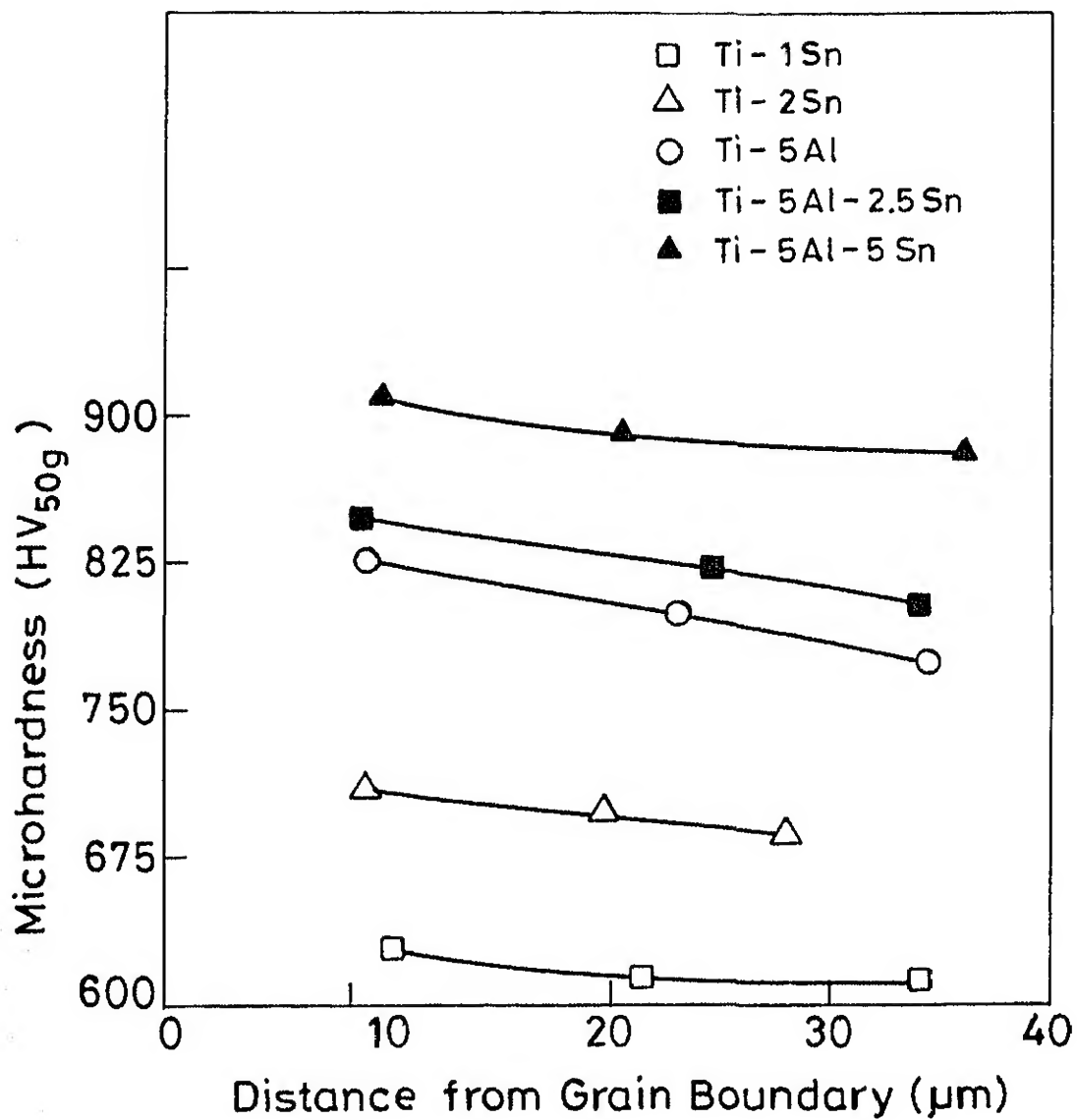


Fig.5.9 Microhardness variation of different sintered Ti-base alloys.

5.2. Transient Liquid Phase Sintered $\alpha + \beta$ Titanium Alloys

The results obtained from TLPS of $\alpha + \beta$ Ti-6 Al-6 V-xSn ($x = 0, 1, 2, 3$) alloys have been given in the following sections.

5.2.1. Densification

The variation of sintered density of Ti-6 Al-6 V-xSn ($x = 0, 1, 2, 3$) alloys with respect to the tin content and the sintering temperature has been shown in Figure 5.10. It is clear from this figure that the sintered density increases with increase in volume fraction of the liquid forming element tin. The amount of volume fraction of liquid in different Ti-6 Al-6 V-xSn alloys has been shown in Table 5.3. Also, it is clear that sintering at 1300°C (1573 K) gives better sintered density in these alloys as compared to the alloys sintered at 1200°C (1473 K).

Volume fractions of interconnected, closed and total porosities of the alloys sintered at 1300°C (1573 K) against their tin content are shown in Figure 5.11. It can be seen that the volume fraction of closed and total porosities decrease with increase in tin content of the alloy.

5.2.2. Microstructural Development

Optical micrographs of the sintered and homogenized Ti-6 Al-6 V, Ti-6 Al-6 V-1 Sn, Ti-6 Al-6 V-2 Sn and Ti-6 Al-6 V-3 Sn have been shown in Figures 5.12, 5.13, 5.14 and 5.15 respectively. It can be seen that the addition of tin is not showing any difference in the microstructure. The alloys in the as-sintered condition reveal α in equiaxed and platelet forms

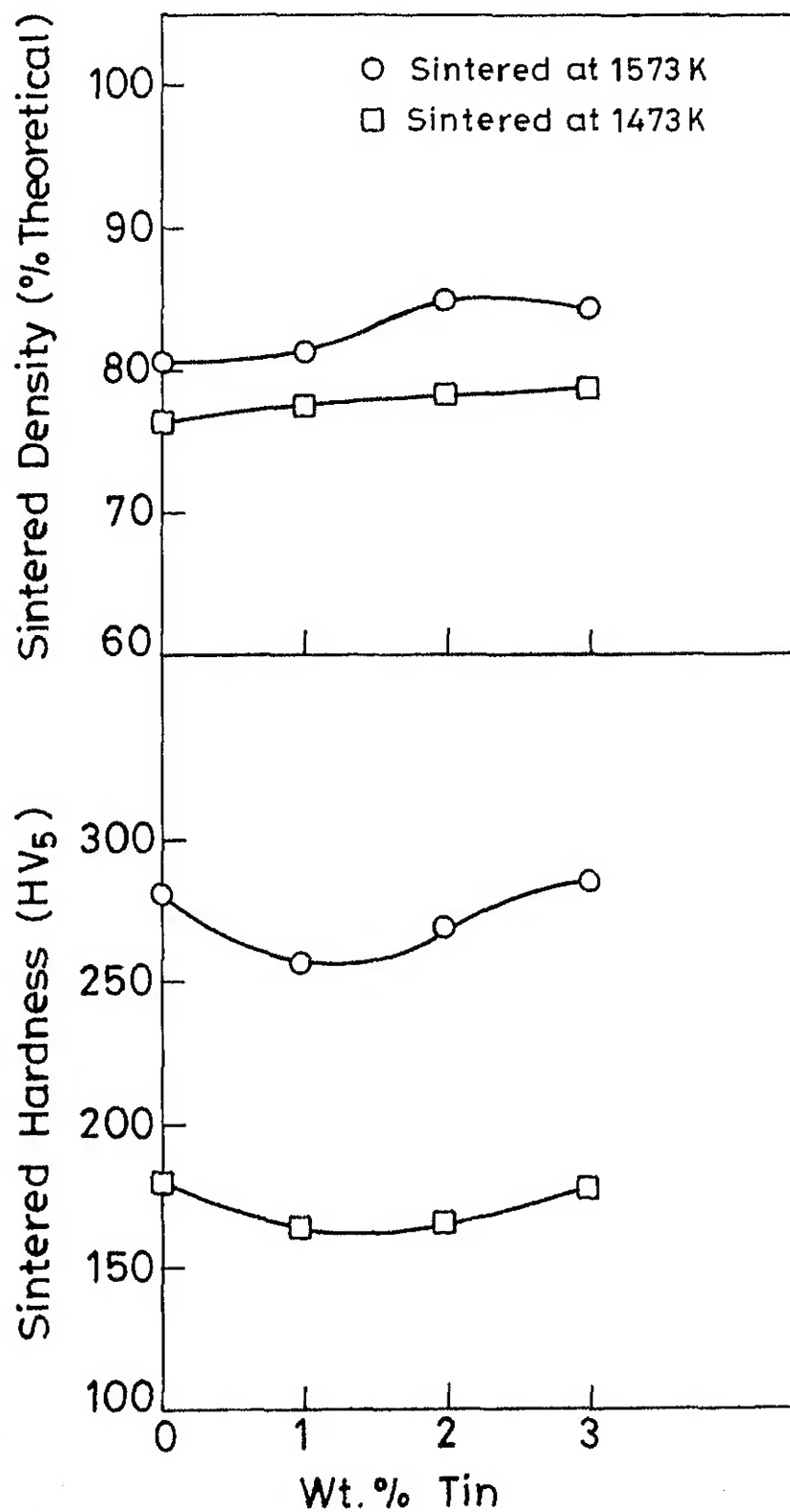


Fig. 5.10 Variation of sintered density and Vickers hardness with respect to the tin content and sintering temperature of Ti-6Al-6V-x Sn (x=0, 1, 2, 3) alloys.

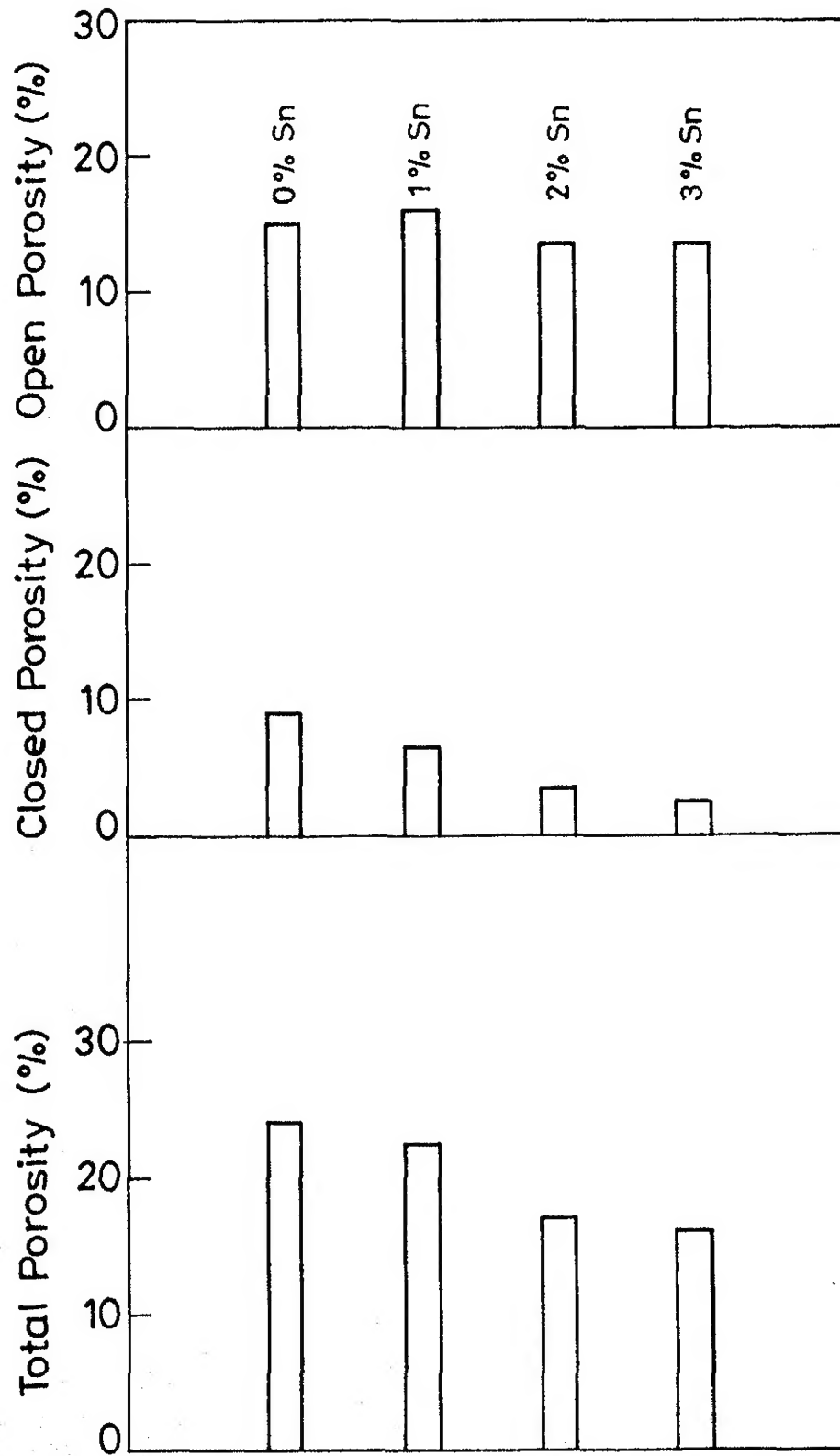
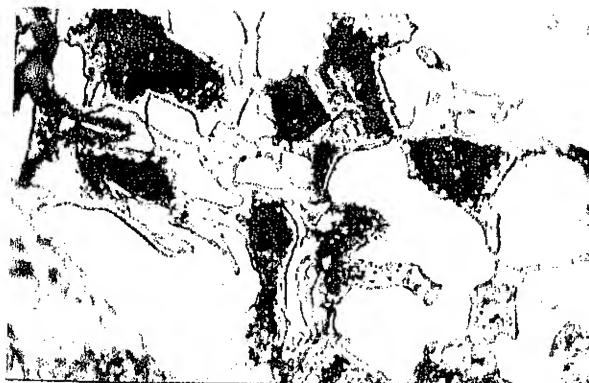
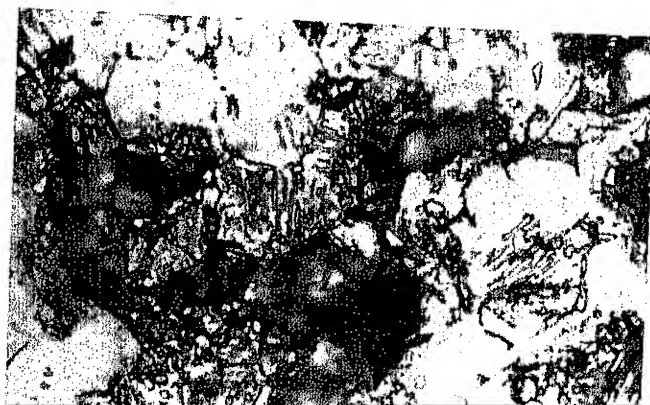


Fig.5.11 Variation of different types of porosities in Ti-6Al-6V-xSn (x=0, 1, 2, 3) alloys.



(a)



(b)



(c)

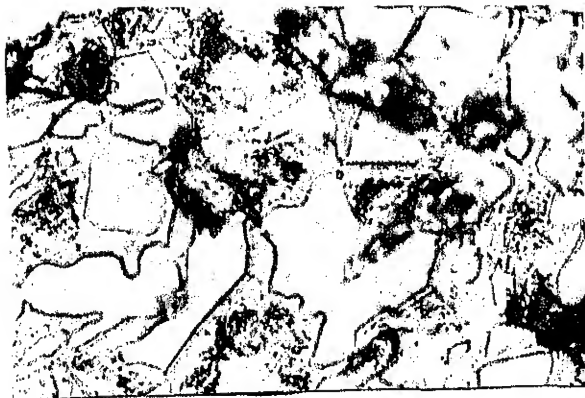
Figure 5.12. Optical micrographs of Ti-6 Al-6 V alloy in the (a) as-sintered, (b) homogenized at 1000°C for 4 hr and (c) homogenized at 1000°C for 20 hrs conditions. 850



(a)



(b)



(c)

Figure 5.13. Optical micrographs of Ti-6 Al-6 V-1 Sn alloy in the (a) as-sintered, (b) homogenized at 1000°C for 4 hrs and (c) homogenized at 1000°C for 20 hrs. 500X



(a)



(b)

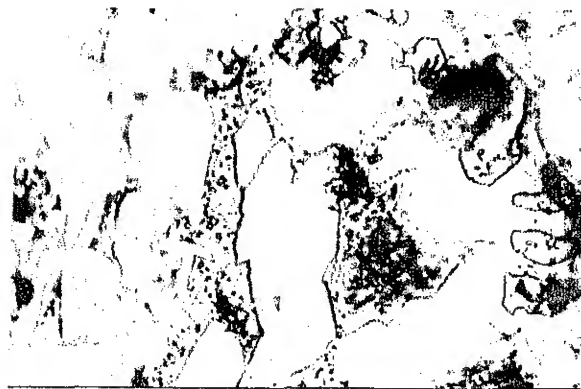


(c)

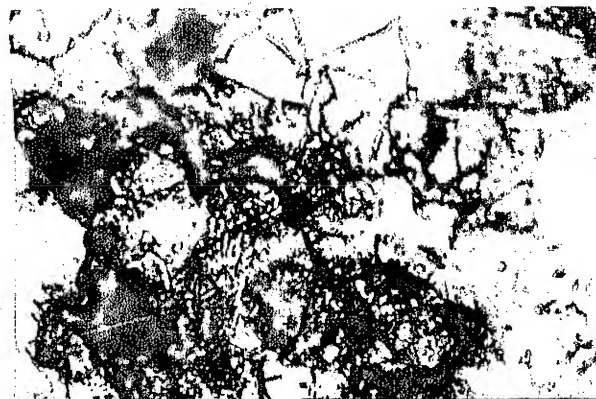
Figure 5.14. Optical micrographs of Ti-6 Al-6 V-2 Sn alloy in the (a) as-sintered, (b) homogenized at 1000°C for 4 hrs and (c) homogenized at 1000°C for 20 hrs. 850X



(a)



(b)



(c)

Figure 5.15. Optical micrographs of Ti-6 Al-6 V-3 Sn alloy in the (a) as-sintered, (b) homogenized at 1000°C for 4 hrs and (c) homogenized at 1000°C for 20 hrs. 850X

TABLE 5.3. Typical EDAX results of Ti-6 Al-6 V-xSn (x = 0, 1, 2, 3) alloy in (1) as sintered at 1300°C for 1 hr, (2) as-sintered and homogenized at 1000°C for 4 hrs and (3) as-sintered and homogenized at 1000°C for 20 hrs conditions

Tin content, wt %	Analysis (wt %) of alloys in conditions			
	Element	1	2	3
0	Ti	62.0-89.3	76.1-93.2	83.2-92.1
	Al	3.9-13.8	4.2-11.9	3.8-8.6
	V	2.7-14.2	2.9-12.2	4.7-9.3
1	Ti	63.2-91.2	79.1-91.7	79.8-89.0
	Al	4.1-14.9	3.8-10.4	4.1-9.6
	V	2.1-16.2	4.3-9.2	3.9-7.2
	Sn	0.1-3.1	0.3-3.3	0.6-2.3
2	Ti	63.4-90.1	65.8-88.9	81.2-87.8
	Al	3.9-16.2	4.6-9.9	4.1-9.8
	V	3.2-11.9	5.6-11.1	5.4-8.9
	Sn	0.4-4.1	0.7-3.8	0.7-3.1
3	Ti	80.2-93.1	81.2-91.2	80.1-91.4
	Al	2.7-12.9	4.8-8.9	4.1-7.9
	V	4.5-13.6	3.8-10.1	3.8-8.4
	Sn	0.2-3.7	0.9-5.2	0.8-3.7

in addition to equiaxed β . With increase in the homogenization period, the β -phase partially decomposes into α -phase, with the resultant decrease in the volume fraction.

SEM micrographs of the sintered and homogenized alloys taken at lower magnifications are shown in Figure 5.16 from which it is evident that the pores get rounded in the homogenized alloys. Typical features observed under SEM at higher magnification of these alloys showing the α -plates and the equiaxed α grains have been shown in Figure 5.17.

Typical results obtained from EDAX of the as-sintered and homogenized alloys are summarized in Table 5.4. It can be observed from these results that composition range of individual alloying elements gets narrowed down with increase in the homogenizing period.

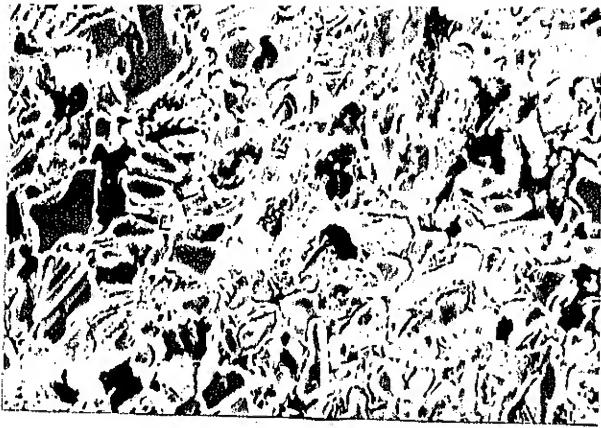
5.2.3. Hardness of Alloys

Macrohardness obtained after sintering of the Ti-6 Al-6 V-xSn alloys with respect to the tin content and the sintering temperature has been shown in Figure 5.10. It can be observed that increase in sintering temperature increases the sintered hardness. Hardness of the sintered alloy decreases with tin addition, but it increases with increase in tin content.

5.3. HIP'ed Ti-6 Al-4 V Alloy

The density of HIP'ed Ti-6 Al-4 V alloy was found to be 99.6% of the theoretical density. The microstructural examination of the unetched samples showed a few micropores.

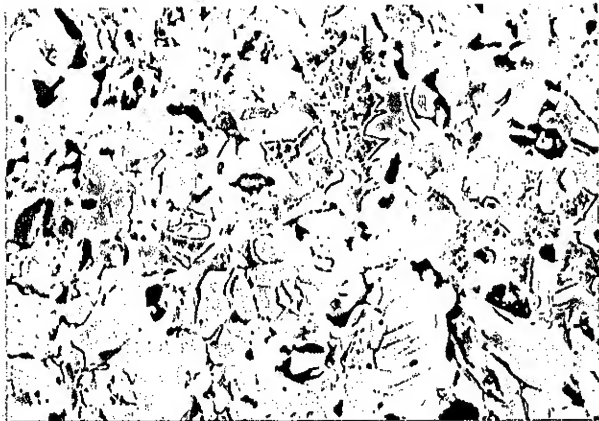
Tensile strength, yield strength, % elongation, % reduction in area and Vickers hardness variation of the Ti-6 Al-4 V



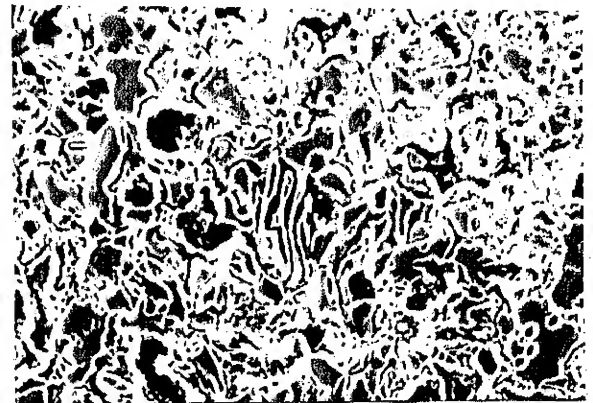
(a)



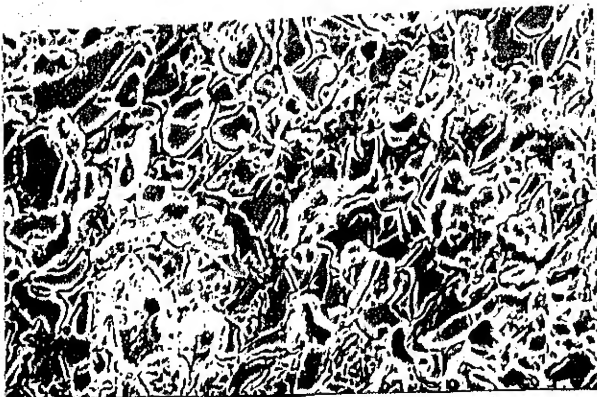
(b)



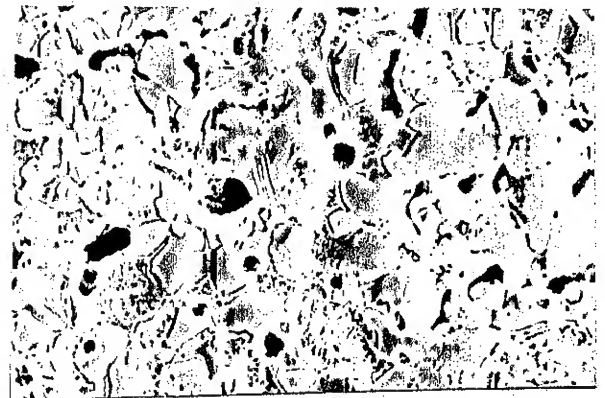
(c)



(d)



(e)



(f)

Figure 5.16. SEM micrographs of Ti-6 Al-6 V (a,c,e) and Ti-6 Al-6 V-2 Sn (b,d,f) alloys showing pore morphology in the as-sintered (a,b), homogenized at 1000°C for 4 hrs (c,d) and for 20 hrs (e,f). 500X



(a)



(b)

1500X



(c)



(d)

3000X

Figure 5.13. Optical micrographs of Ti-6 Al-6 V-1 Sn alloy in the (a) as-sintered, (b) homogenized at 1000°C for 4 hrs and (c) homogenized at 1000°C for 20 hrs.

TABLE 5.4. Volume fractions of liquid in various Ti-6 Al-6 V-xSn alloys

Composition	Volume fraction of liquid (%)
Ti-6 Al-6 V-0 Sn	3.4
Ti-6 Al-6 V-1 Sn	4.1
Ti-6 Al-6 V-2 Sn	4.9
Ti-6 Al-6 V-3 Sn	5.6

alloy in the as HIP'ed and the two heat treated conditions are shown in Figure 5.18. The figure reveals that there is not much difference in the properties of the annealed and the as-HIP'ed alloy. However, there is noticeable increase in the ductility, strength and hardness of the solution treated and overaged alloy, compared to the HIP'ed and annealed alloys.

Optical micrographs and SEM fractographs of the HIP'ed Ti-6 Al-4 V alloy have been shown in Figure 5.19. Optical micrographs of the HIP'ed and annealed alloys show widmanstatten α -plates in a matrix of β -phase, the amount of β -phase increasing in the annealed and air cooled alloy compared to the HIP'ed alloy. Solution treated and overaged alloy shows primary α plates along with equiaxed α -grains in a tempered martensite matrix. Fractographs of the HIP'ed and heat treated Ti-6 Al-4 V shows ductile fracture with relatively uniform and fine dimpled structure in case of solution treated and overaged alloy.

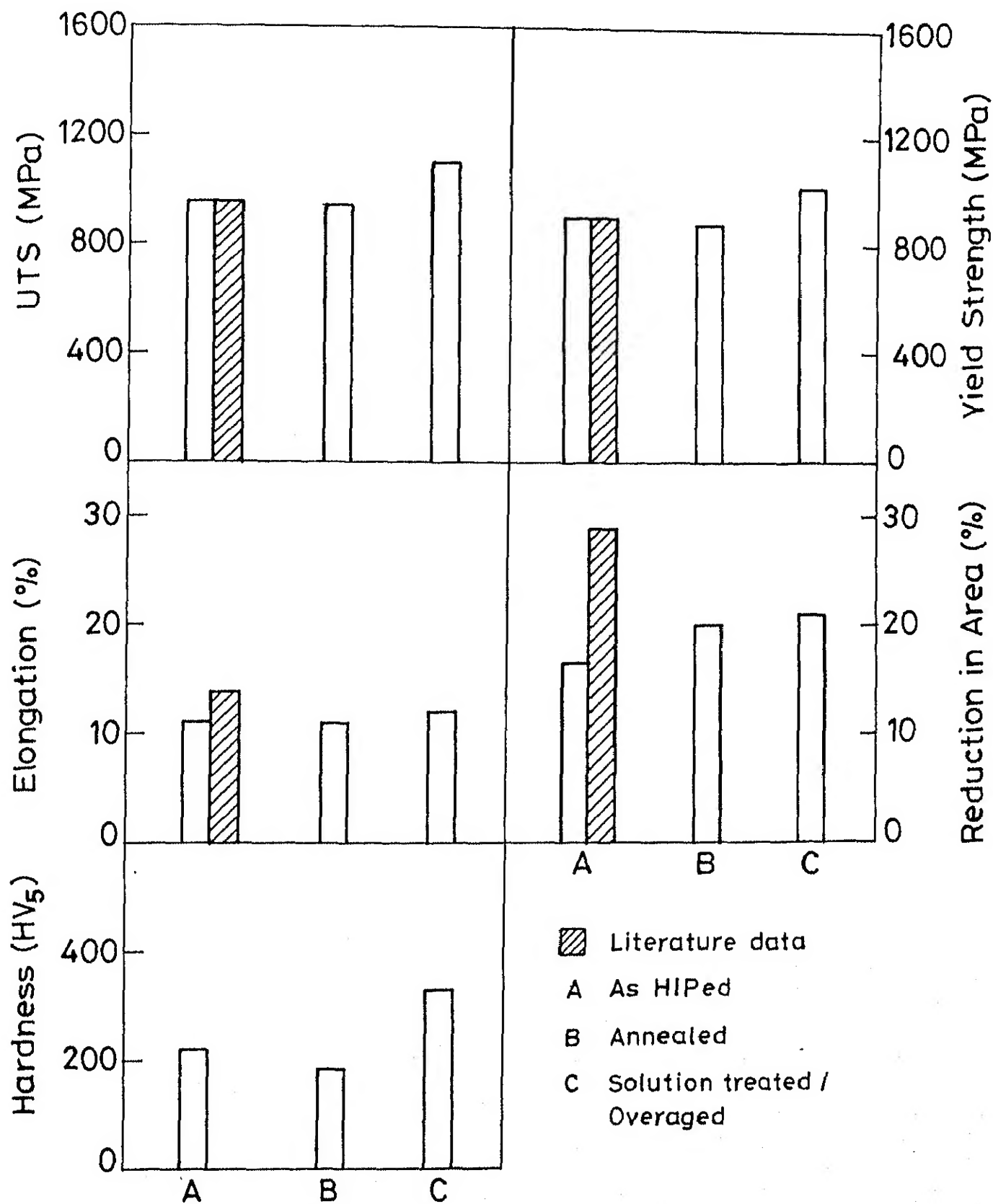
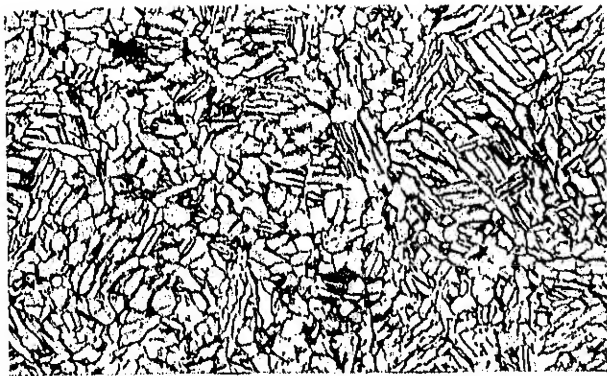


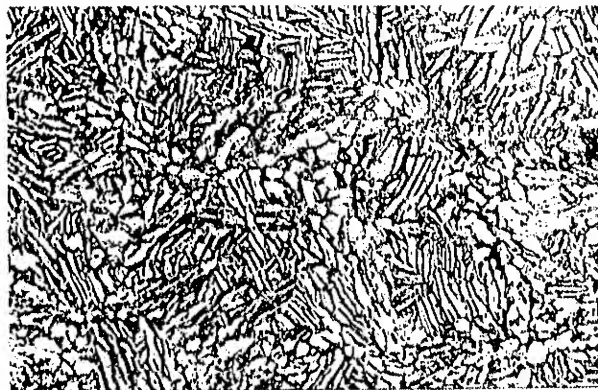
Fig. 5.18 Mechanical properties of Ti-6Al-4V alloys in HIP'ed and HIP'ed/heat treated conditions.



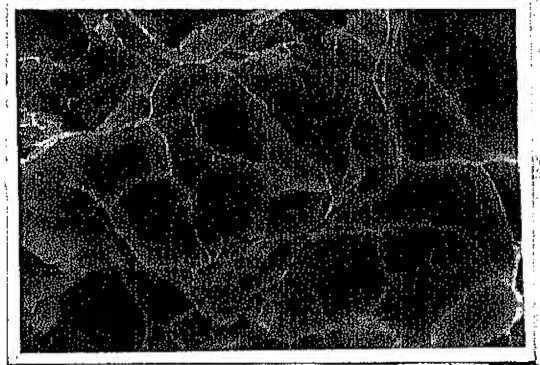
(a)



(d)



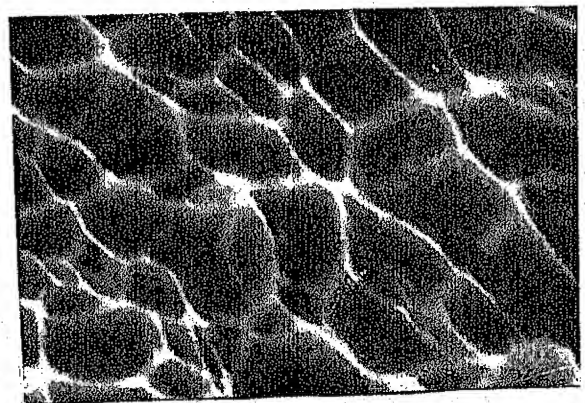
(b)



(e)



(c)



(f)

200X

1000X

Figure 5.19. Optical micrographs and SEM fractographs of Ti-6 Al-4 V after HIP'ing (a,d) after annealing (b,e) and after solution treating and overaging (c,f).

CHAPTER - 6

DISCUSSION

6.1. Transient Liquid Phase Sintering (TLPS) of Ti-Al, Ti-Sn and Ti-Al-Sn Alloys

The results obtained on TLPS studies of the Ti-Al, Ti-Sn and Ti-Al-Sn are discussed below.

6.1.1. Densification

Sintering behaviour of binary and ternary alloys of titanium studied in the present work can be explained in terms of TLPS occurring in these systems. Like in the persistent liquid phase sintering (PLPS), the liquid in the TLPS is also drawn into the pores of the solid by capillary forces. Wetting characteristics and the amount of liquid forming additives are important variables which can substantially change the course of sintering kinetics, microstructural evolution and sintered properties. In TLPS, however, green compacts made from premixes of elemental powders are not in the chemical equilibrium, the equilibrium being attained only during prolonged sintering. There is, therefore, all likelihood that all the phases in the phase diagram of the system found at the sintering temperature appear at some time or the other. These phases, however, will be thermodynamically unstable and transient in nature. Thus, the course of TLPS is considerably affected by the chemical composition of the liquid and other transient phases formed during sintering. The occurrence of the liquid as well as other transient phases is governed by the phase boundaries in the phase

diagram of the system. Further, since energies of alloy or intermetallic compound formation (chemical driving forces) are normally some magnitudes higher than those associated with the reduction of surfaces, i.e. the decreasing of porosity, it is thermodynamically possible that the porosity of compacts is increased rather than decreased [54].

An examination of phase diagrams of Ti-Al and Ti-Sn systems (Figure 6.1) [55] shows that the liquid phase forming during both alloy groups will be that of liquid aluminium and liquid tin at their respective melting points. Both of them have good wetting characteristics and hence they will be able to penetrate the inter/intra-particle pores and also the grain boundaries. The process of TLPS occurring in various binary titanium alloys can, therefore, be thought of occurring in the following stages,

1. Melting of all aluminium/tin particles,
2. Grain boundary penetration by aluminium/tin melt,
3. Interdiffusion of Ti and Al/Sn at the liquid-solid interface,
4. Shrinkage of the compact due to the capillary forces exerted by the melt.

These stages of TLPS in binary Ti-Al/Sn alloys have been schematically shown in Figure 6.2.

Further, examination of Ti-Al and Ti-Sn phase diagrams shows that they are characterized by the presence of intermetallics viz. Ti_3Al , $TiAl$ and Al_3Ti in the Ti-Al system and Ti_3Sn , Ti_2Sn , Ti_5Sn_3 and Ti_6Sn_5 in the Ti-Sn system. Sintering of various Ti-Al and Ti-Sn alloys at $1300^{\circ}C$ (1573 K) therefore implies the formation of these intermetallics during their TLPS

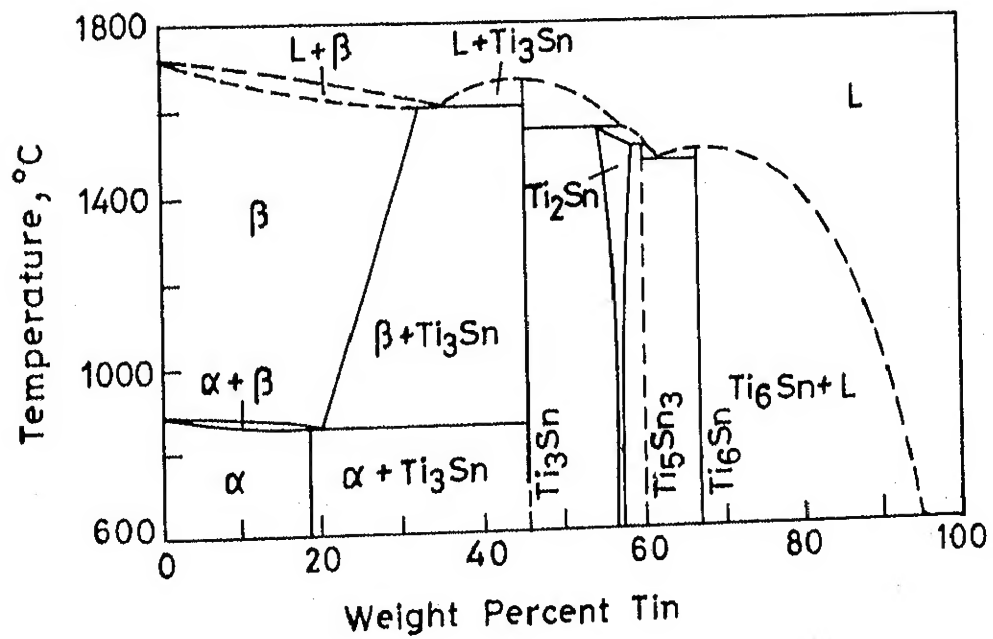
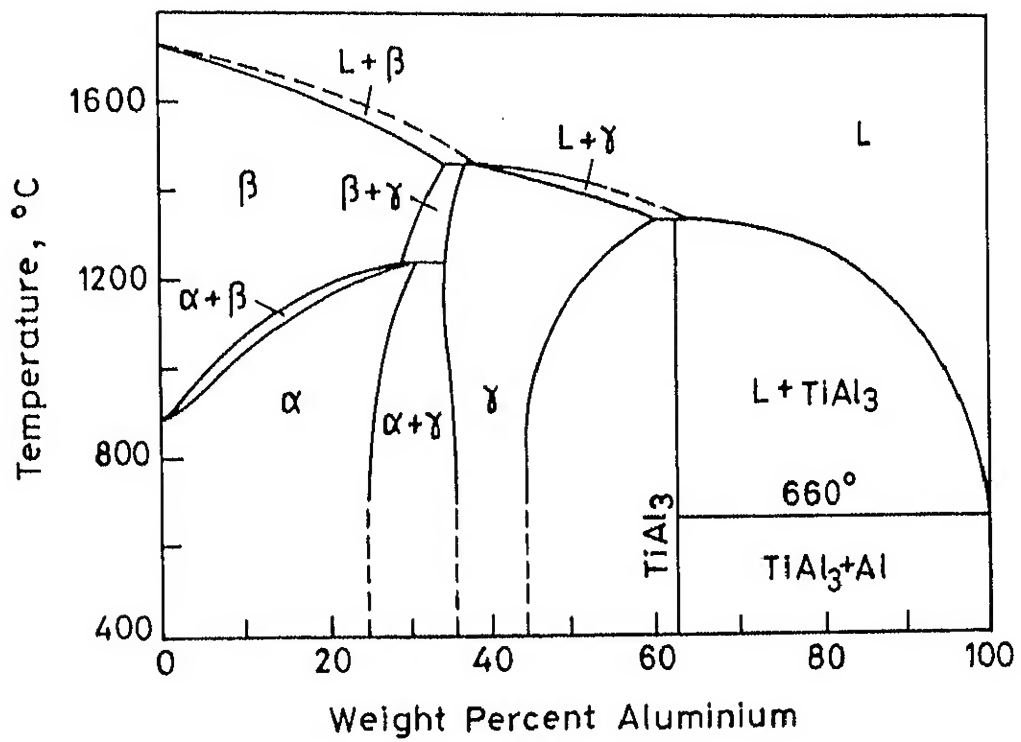


Fig.6.1 Binary phase diagrams of Ti-Al and Ti-Sn systems [55].

through only for a limited period. Formation of intermetallic compounds is known to be highly exothermic [56] and as pointed out by Savitskii [47], this factor alone can cause growth of the compacts during their TLPS. Sintering behaviour of Ti-36 Al, Ti-6 Al and Ti-6 Sn alloys has been studied by Savitskii et al. [47] and Khromov [51]. Dilatometric studies of Savitskii et al. showed that the formation of intermetallic compound during TLPS of Ti-36 Al alloy compacts was associated with intense heat evolution and extensive compact growth. Similarly results of Khromov on isothermal sintering of Ti-6 Al alloy carried out at 1100°C (1373 K) revealed that the compact growth occurred during early stages of sintering. The extent of growth and the period over which it persisted were found to increase with green density of compacts. The growth occurring in Ti-6 Sn alloy, however, was found to be much less than that in Ti-6 Al alloy. An increase in sintered density of compacts of various Ti-Al, Ti-Sn and Ti-Al-Sn alloys, as shown in Figure 5.1 must therefore be viewed as a superimposition of initial compact growth followed by shrinkage. The observed difference in growth behaviour of Ti-Al and Ti-Sn system by these authors [47,51] can be attributed to the following,

- (i) the difference in solubility of titanium in liquid aluminium and liquid tin,
- (ii) the difference in enthalpy of reactions of formation of Ti-Al and Ti-Sn intermetallic compounds,
- (iii) the difference in densities of intermetallic compounds of Ti-Al and Ti-Sn,
- (iv) volumetric changes which occur in aluminium and tin due to their melting,

- (v) the difference in the dihedral angles of liquid tin and liquid aluminium with solid titanium particles,
- (vi) the difference in Kirkendall porosities formed in the two systems.

Apart from higher enthalpies of reaction for the formation of Ti-Al compounds than those of Ti-Sn compounds [57], titanium has negligible solubility in liquid aluminium and has a solubility of 5% in liquid tin at 600°C (873 K). As a consequence of diffusion of aluminium atoms from liquid melt to solid titanium the particle size of the latter grows. On the other hand, solubility of titanium in liquid tin implies that the particle size of the former decreases during TLPS of Ti-Sn alloys. On this account, therefore, the compacts of Ti-Al must grow while those of Ti-Sn alloys must shrink. Similarly, since the densities of Ti-Al intermetallics are lower, and those of Ti-Sn intermetallics are higher than that of titanium there will be a tendency for growth in Ti-Al alloy and shrinkage in Ti-Sn alloy compacts. Finally, both aluminium and tin expand after their melting but volumetric changes (+6.3% for Al and +2.7% for Sn [51]) occurring in the former are more than twice in the latter. While all the factors discussed above favour compact growth in Ti-Al alloys, the situation in Ti-Sn alloys appears to be governed by opposite contributions. Due to these contributions of opposite nature the compact growth in Ti-Sn alloys would be considerably lower than that in Ti-Al alloys. This explains the substantial difference in growth behaviour of Ti-6 Al and Ti-6 Sn alloys studied by Khromov [51] and also the results of the present study (Figure 5.2) suggesting that the

rate of densification with respect to the volume fraction of available liquid phase is higher in Ti-Sn alloys than in the case of Ti-Al alloys.

The role of tin and aluminium in ternary Ti-Al-Sn alloys during their TLPS appears to be synergetic. Though, no detailed examinations of ternary phase diagrams of Ti-Al-Sn system has been reported [58], the examination of phase diagram of Al-Sn suggests that the liquid to appear first in these alloys will be Al-Sn eutectic at 230°C (500 K) temperature. Also, the densities of intermetallics formed in Ti-Al-Sn system will be higher than that of Ti-Al system. Compact growth occurring in Ti-Al-Sn system will therefore be lower than that of Ti-Al alloys. Apart from these reasons, the enhanced shrinkage occurring in Ti-Al-Sn alloys can be attributed to (i) an increase in the volume fraction of the melt, (ii) a fall in the melting point of aluminium in the presence of tin giving rise to an effectively less viscous melt during sintering which aids in better pore filling characteristics, (iii) a decrease in the surface tension of aluminium melt in the presence of tin [59] which promotes a better melt spreading and (iv) ideal wetting of molten tin over aluminium since the contact angle is 0° [60].

A comparison of the pore size distribution in various sintered alloys (Figure 5.5) with the size distribution of tin and aluminium particles (Figure 4.1) suggests that the mechanism of formation of new system of pores as suggested in Figure 6.2, is indeed realistic. Further, the dissolution of titanium in liquid tin and diffusion of aluminium from its melt to solid titanium implies that the pore channel dimensions increase in

Ti-Sn alloys and decrease in Ti-Al alloys during their TLPS. The porosity left behind after the sintering, has a higher volume fraction of interconnected pores in the former and closed pores in the latter. This explain the results shown in Figure 5.6.

6.1.2. Microstructural Development

Microstructural development in TLPS of binary Ti-Al/Ti-Sn alloys can be understood from the proposed stages of TLPS occurring in these systems as shown in Figure 6.2. Examination of Ti-Al and Ti-Sn phase diagrams shows that they are characterized by the presence of intermetallics viz. Ti_3Al , $TiAl$ and Al_3Ti in the Ti-Al system and Ti_3Sn , Ti_2Sn , Ti_5Sn and Ti_6Sn_5 in the system. Sintering of various Ti-Al and Ti-Sn alloys at 1573 K therefore implies the formation of these intermetallics during their TLPS though only for a limited period. From the results obtained on Ti-5 Al and Ti-5 Al-5 Sn samples sintered at 660°C (933 K) for 15 min (0.9 ks) it is clear that formation of intermetallics occurs at few places of these samples (Figure 5.7, Table 5.2).

Since the solubility of titanium in liquid tin implies that the particle size of the former decreases during TLPS of Ti-Sn alloys. On the other hand due to the negligible solubility of titanium in liquid aluminium, diffusion of aluminium atoms from liquid melt to solid titanium takes place and hence the particle size of titanium increases. Results obtained from grain size measurement of different alloys shown in Table 5.1 support such an argument.

6.1.3. Hardness of the Alloys

Variations in hardness values of various sintered alloys can be explained in terms of

- (a) solid-solution strengthening of α -phase of titanium by its alloying,
- (b) reduction of porosity of green compacts during their TLPS,
- (c) grain size of different alloys in as-sintered condition.

Both aluminium and tin have similar type of electronic configurations for their valency electrons and thus are preferentially dissolved in the hcp structure of the α -phase of titanium [61]. Collings has discussed the strengthening of titanium by binary alloying additions in α -phase in terms of strong, local and directional bonds formed between the solute and the solvent atoms [62]. Furthermore, it has been suggested that the strengthening effect of α stabilizers in ternary alloys of titanium is expected to be synergetic. According to the stable electron configuration model proposed by Samsanov [61] the stability of sp^3 configuration of aluminium is higher than that of tin which is evident from the relatively high hardness of the former. Samsanov's model also justifies the definition of Rosenberg's aluminium equivalent, Al^* , in titanium alloys where

$$Al^* = Al + \frac{1}{3} Sn + \frac{1}{6} Zr + 10 (O^*) \quad [63]$$

where all the percentages in weights and O^* represents the equivalent oxygen content defined as

$$O^* = O + C + 2N$$

It has already been discussed that the microhardness

data within the interior of different grains (Figure 5.9) showed that the alloying additions were properly homogenized in the as-sintered alloys. A higher hardness of alloys containing aluminium can therefore, be understood in terms of higher solid solution strengthening of titanium due to alloying with aluminium.

A plot between the sintered hardness and Rosenberg's aluminium equivalent of different alloys has been shown in Figure 5.8. As grain sizes of different alloys were found to be of the same order of magnitude, a steep rise in the hardness of ternary Ti-Al-Sn alloys can be explained in terms of the synergistic effect of aluminium and tin in reducing the porosity of Ti-Al-Sn compacts during TLPS.

6.2. Transient Liquid Phase Sintering of Ti-6 Al-6 V-xSn (x = 0, 1, 2, 3) Alloys

6.2.1. Densification

Densification process occurring in the presently studied Ti-6 Al-6 V-xSn alloys can be explained in terms of transient liquid phase sintering.

Sintering kinetics and microstructural developments of these alloys are functions of various factors like the volume fraction of liquid, wetting of the liquid on the solid powder particles, solubility of solid phase in the liquid, diffusivities of the constituent elements in the system and heating and cooling rates followed during sintering. The densification during the transient liquid phase sintering of Ti-Al-V-Sn alloys occurs in the following steps:

1. Melting of aluminium/tin powder particles.

2. Wetting of the solid titanium and V-Al master alloy particles and their grain boundary penetration by aluminium/tin melt.
3. Shrinkage of the compact due to the capillary forces exerted by the melt.
4. Dissolution of titanium in the melt thus contributing to the solution-reprecipitation stage of liquid phase sintering.

Literature data [60] suggests that aluminium and tin melts have good wetting over titanium. From the binary phase diagram of V-Al, it can be observed that 61 V-39 Al master alloy remains in the solid state at the selected sintering temperature [64]. The overall wettable liquid formed is thus utilized in filling up the interparticle and intra-particle pores of titanium and V-Al master alloy. The increase in density of various alloys of this system, is, therefore, dependant on the volume fraction of the liquid. This is confirmed by the present results, as the density of the sintered compact increases with increase in the melt volume fraction (Table 5.3, Figure 5.10).

6.2.2. Microstructural Development

Optical micrographs of sintered Ti-6 Al-6 V-xSn alloys (Figures 5.12-5.15.a) show equiaxed α and β grains and some amount of α -plates. An observation of β -grain in the as sintered and partially homogenized alloys (Figures 5.12-5.15.a,b) infers that there is composition gradient at the grain boundary. During the sintering and homogenizing processes, vanadium in the master alloy stabilizes the β -titanium whereas aluminium and tin

in the premix and aluminium from the master alloy stabilize the α -titanium. The resulting microstructural features, therefore, depends on the compositional distributions of different alloying elements. From the diffusivity data obtained from different sources [65,66], it is apparent that the diffusivity of vanadium in titanium ($14.9 \times 10^{-9} \text{ cm}^2/\text{s}$) at the sintering temperature for this particular alloy concentration is about two times that of aluminium ($8.77 \times 10^{-9} \text{ cm}^2/\text{s}$) while the diffusivity of tin ($3.4 \times 10^{-9} \text{ cm}^2/\text{s}$) is the lowest among all the alloying additives. This feature is confirmed by the EDAX analysis results (Table 5.4), which shows a narrower range of composition distribution of vanadium as compared to aluminium. The enhanced sinterability of Ti-6 Al-6 V premix after tin addition is also attributed to the fact that titanium is more soluble in liquid tin (5% at 873 K) as compared to its negligible solubility in molten aluminium [55]; a fact which promotes solution-precipitation stage of liquid phase sintering.

The microstructures of the investigated Ti-6 Al-6 V-xSn alloys do not show α -phase as completely widmanstatten structure (Figure 5.12), which may be due to the incomplete dissolution of V-Al master alloy particles during sintering. It is apparent that the distribution of the α -phase within the β -phase is not uniform in the as-sintered alloys (Figure 5.12.a) or alloys homogenized for a relatively less period (Figure 5.12.b). This feature is also confirmed by EDAX results. However, after a prolonged homogenization treatment (72.0 ks at 1273 K), the investigated alloys reveal a homogeneous microstructure consisting of plate-like and equiaxed α -grains and equiaxed β -grains (Figures 5.12-5.15.c).

6.2.3. Hardness of the Alloys

The effect of alloying elements on the hardness of elemental titanium can be seen from the Vickers hardness variation in Ti-6 Al-6 V-xSn alloys (Figure 5.10). Collings [62] has explained this on the basis of formation of strong, local and directional bonds between the solute and surrounding titanium atoms. It was also established that the role of sp elements like aluminium and tin on hardening of titanium is more pronounced than the transition element viz. vanadium.

6.3. HIP'ing of Ti-6 Al-4 V Alloy

The microstructural development in an $\alpha + \beta$ titanium alloy depends on both the thermal and mechanical processing sequences [67]. In cases, where the finishing or solution treatment temperatures are above the β -transus, the microstructures consist of widmanstätten $\alpha + \beta$ or α' depending on the cooling rate. The microstructure of HIP'ed as well as annealed Ti-6 Al-4 V studied presently consists of widmanstätten α plates in a β -matrix. As the width of α -plates in annealed alloy is relatively smaller compared to that of as-HIP'ed alloy, it can be inferred that due to a relatively faster cooling rate i.e. air cooling followed in the annealed alloy, an increase in the amount of β -phase results. The microstructure developed in Ti-6 Al-4 V after water quenching consists of primary α and martensite α' . Overaging gives rise to a structure of primary α in a matrix of tempered martensite α' (Figure 5.19). Such a treatment imparts good strength as well as ductility since the microstructure consists of primary α in a tempered martensite [68]. The present

results obtained from the tensile tests confirm the trend expected as a sequence of different heat treatments. Comparison of the mechanical properties obtained for the presently studied HIP'ed alloy after annealing with the results of Shienker et al. [36] shows the similarities in the values (Figure 5.18).

The SEM fractographs of Ti-6 Al-4 V alloy in different heat treated conditions (Figure 5.19), exhibit ductile fracture in solution treated/overaged alloys showing relatively uniform and fine dimpled structure. It is known that in microstructures containing equiaxed α in a tempered α' or aged β matrix, α -particles play an important role in determining the ductility. It is observed that during fracture voids form at the equiaxed α /tempered α' interfaces. It has been proposed [68] that the ease of void growth depends upon the spacing of the α -plates which act as obstacles to its growth resulting in greater strain to fracture. In the case of HIP'ed and annealed alloys, as per expectation [67], fracture occurs along the α/β interface in addition to prior β -grain boundaries.

CHAPTER - 7

CONCLUSIONS

Transient liquid phase sintering behaviour of binary Ti-Al, Ti-Sn, ternary Ti-Al-Sn and quaternary Ti-Al-V-Sn alloys proposed through premix route appears to be quite complex. On the basis of the results obtained in the present investigation the following conclusions can be drawn:

1. An increase in the density of compacts of binary and ternary titanium alloys based on the compositions of Ti, Al and Sn can be viewed as a superimposition of initial compact growth and subsequent shrinkage. Theoretical considerations suggest that the compact growth in binary Ti-Al alloys is expected to be higher than that in binary Ti-Sn and ternary Ti-Al-Sn alloys.
2. The densification of green compacts of various titanium alloys during their transient liquid phase sintering increases with increasing the volume fraction of the liquid phase. However, the rate of densification with respect to the available liquid is higher in Ti-Sn and Ti-Al-Sn alloys than in Ti-Al alloys.
3. The effect of tin and aluminium in ternary Ti-Al-Sn alloys on the densification during their transient liquid phase sintering is synergetic.
4. Sintered Ti-Sn alloys contain higher interconnected porosity compared to Ti-Al alloys. The volume fraction of interconnected porosity in Ti-Sn alloys increases by

increasing the percentage of tin.

5. Aluminium has more pronounced effect than tin in increasing the sintered hardness of titanium. A steep rise in the hardness v/s Rosenberg's aluminium equivalent curve, found at different compositions of alloys, can be explained due to synergetic effect of aluminium and tin on the densification rate of sintered compacts.
6. For any selected composition of Ti-6 Al-6 V-Sn (0-3) alloys prepared by transient liquid phase sintering, sintered properties were improved with increase in the sintering temperature.
7. Both equiaxed and plate like α -grains and β -grains were obtained in the microstructure of Ti-6 Al-6 V-Sn (0-3) alloys probably due to the incomplete dissolution of the V-Al master alloy.
8. The mechanical properties of prealloyed Ti-6 Al-4 V alloy after hipping were comparable with those of literature data. Solution treating/water quenching followed by overaging of the alloys gave rise to superior properties compared to those of as-HIP'ed or annealed ones.

CENTRAL LIBRARY
I. I. T., KANPUR

Acc. No. A. 110759

REFERENCES

1. M.J. Donachie, Jr., in 'Titanium and Titanium Alloys', Ed. M.J. Donachie, Jr., ASM, Ohio, 1982, p. 3.
2. S.L. Semiatin and T. Altan, Isothermal and Die Forging of High Temperature Alloys, MCIC-83-47, Metals and Ceramic Informations Centre, Ohio, 1983.
3. C.C. Chen and J.E. Coyne, in 'Titanium '80', eds. H. Kimura and O. Izumi, The Metallurgical Society of AIME, Warrendale, 1980, p. 2513.
4. E.L. Thellman, Powder Metallurgy International, Vol. 11, No. 2, 1979, 47.
5. F.H. Froes and J.R. Pickens, J. Met., 1984, Vol. 36, No. 1, 14.
6. S.H. Wrang, J. Mater. Sci., 1986, Vol. 21, 2224.
7. S.J. Savage and F.H. Froes, J. of Metals, 1984, Vol. 36, 20.
8. S. Abkowitz, J.M. Siergiej and R.D. Regan, in 'Modern Developments in Powder Metallurgy', Ed. H.H. Hausner, Plenum Press, New York, 1971, p. 501.
9. R.F. Lynch, in 'Progress in Powder Metallurgy 1972', Ed. A.S. Bufferd, MPIF, New York, 1972, p. 179.
10. K. Akechi and Z. Hara, Powder Metallurgy, 1981, No. 1, 41.
11. A.L. Borisova and Yu. N. Kopichev, Soviet Powder Metallurgy and Metal Ceramics, 1977, Vol. 16, No. 11, 849.
12. V.A. Pavlov and G.V. Avrunina, Soviet Powder Metallurgy and Metal Ceramics, 1978, Vol. 17, No. 2, 155.
13. M. Igharo and J.V. Wood, Powder Metallurgy, Vol. 28, No. 3, 1985, 131.
14. F.H. Froes and J.R. Pickens, J. Met., Vol. 36, No. 1, 1984, 14.
15. F.H. Froes, D. Eylon, G.E. Eichelman and H.M. Burte, J. Met., Vol. 32, No. 2, 1980, 47.
16. F.H. Froes, D. Eylon and Y. Mahajan, in 'Modern Developments in Powder Metallurgy', Vol. 13, Ed. H.H. Hausner et al., MPIF, Princeton, 1981, 523.
17. G. Welsch, W. Smarsly and R. Borath, Powder Metall. Int., November, 1982, 190.

18. I. Weiss, D. Eylon, M.W. Toaz and F.H. Froes, Met. Trans. A, Vol. 17A, March, 1986, 549.
19. R.R. Boyer, D. Eylon and F.H. Froes, Powder Metall. Int., Vol. 17, No. 5, 1985, 239.
20. J.J. Lucas and P.P. Konieczny, Met. Trans., Vol. 2, 1971, 911.
21. D. Eylon and C.M. Pierce, Met. Trans. A, 7A, 1976, 111.
22. M. Peters, A. Gysler and G. Luetjering, in 'Proceedings of the 5th ICSMA Conference', Aachen, FDR, Vol. 2, 1979, p. 1113.
23. G.R. Yoder, L.A. Cooley and T.W. Crooker, in 'Proceedings of the 23rd Structures and Materials Conference', AIAA, 1982, p. 132.
24. M. Peters, A. Gysler and G. Luetjering, in 'Titanium '80', TMS-AIME, 1980, p. 1777.
25. B. Ferguson, A. Kuhn, O.D. Smith and F. Hofstalter, Int. J. Powder Metall., Vol. 20, No. 2, 1984, 131.
26. H. Jones, 'Rapid Solidification of Metals and Alloys', The Institute of Metals, Monograph No. 8, 1982.
27. H. Jones, J. Mat. Sci., Vol. 19, 1984, 1043.
28. J.V. Wood, Mater. and Design, Vol. 4, 1983, 673.
29. D.H. Ro and M.W. Toaz, in 'Progress in Powder Metallurgy 1982', MPIF/APMI, Vol. 38, 1982, p. 311.
30. A.R.E. Singer, Metals Technology, Vol. 11, 1984, 99.
31. A.R.E. Singer, Met. Mater., Vol. 4, 1970, 246.
32. A.R.E. Singer, J. Inst. Met., Vol. 100, 1972, 185.
33. P.R. Smith, C.M. Cooke, A. Patel and F.H. Froes, in 'Progress in Powder Metallurgy 1982', MPIF/APMI, Vol. 38, 1982, 339.
34. P.R. Smith, C.M. Cooke and F.H. Froes, in 'Materials and Process Continuing Innovations', SAMPE, Vol. 28, 1983, 406.
35. F.H. Froes and D. Eylon, Powder Metall. Int., Vol. 17, No. 4, 1985, 163; No. 5, 235.
36. A.A. Shienker, G.R. Chanani and J.W. Bohlen, Int. J. Powder Metall., Vol. 23, No. 3, 171.
37. D. Eylon and F.H. Froes, Met. Powder Rep., Vol. 41, No. 4, 1986, 287.

38. D. Eylon, T.L. Bartel and M.E. Rosenblum, Metall. Trans., 1980, 11A, 1361.
39. D. Eylon, M.E. Rosenblum and S. Fujishiro, in 'Titanium '80', Science and Technology, Vol. 3, Ed. H. Kimura and O. Izunic, 1980, Warrendale, 1845.
40. D. Eylon and M.E. Rosenblum, Metall. Trans., 13A, 1982, 322.
41. Y.R. Mahajan, D. Eylon, C.A. Kelto, T. Egerer and F.H. Froes, Powder Metall. Int., Vol. 17, No. 2, 1985, 75.
42. F.H. Froes, D. Eylon, G. Wirth, K.J. Grundhoff and W. Smarsly, Met. Powder Rep., 1983, Vol. 38, No. 1, 36.
43. D. Eylon, F.H. Froes, D.G. Heggie, P.A. Blenkinsop and R.W. Gardiner, Met. Trans., 14A, 1983, 2497.
44. R.F. Vaughan, P.A. Blenkinsop and P.H. Morton, in 'AGARD Conf. Proc., No. 200, 1978, p. 11.
45. T.F. Broderick, A.G. Jackson and F.H. Froes, Met. Trans., 1984.
46. A.F. Belov and I.S. Polkin, 'Modern Trends in Titanium Production and Processing', German Metallurgical Society Workshop, University of Nuremberg, Erlanger (July, 1982).
47. A.P. Savitskii and N.N. Burtsev, Soviet Powder Metallurgy and Metal Ceramics, Vol. 18, No. 2, 1979, 96.
48. C. Yixiang, L. Bing and H. Peiyun, in 'W-Ti-Re-Sb '88', Vol. II, Ed. F. Chongune, Pergamon Press, Oxford, 1989, p. 1129.
49. N. Nakamura and Y. Kaieda, Powder Metallurgy, Vol. 31, No. 3, 1988, 201.
50. V.S. Moxson and G.I. Friedman, Metal Powder Rep., Vol. 43, No. 2, 1988, 88.
51. V.G. Khromov, Soviet Powder Metallurgy and Metal Ceramics, Vol. 18, No. 2, 1979, 16.
52. G. Arthur, J. Inst. Metals, Vol. 83, 1954, 1329.
53. Z. Jefferies, Grain Size Measurements, Chem. & Met. Eng., Vol. 18, 1918.
54. A.P. Savitskii, L.S. Marurnova, N.N. Burcev and M.A. Emeljanova, in 'Proc. VII Int. P/M Conf. DDR, Dresden, Vol. 2, 1981, p. 169.
55. E.K. Molchanova, 'Phase Diagrams of Titanium Alloys', Israel Program for Scientific Translations, Jerusalem, 1965, p. 70 and p. 137.

56. P.M. Robinson, in 'Intermetallic Compounds', Ed. J.H. Westbrook, p. 38.
57. I.I. Cornelov, in 'Intermetallic Compounds', Ed. J.H. Westbrook, p. 349.
58. As in Ref. 55, 181.
59. P.C. Mukherjee, 'Fundamentals of Metal Casting Technology', Oxford and IBH, New Delhi, 1979, p. 54.
60. Yu. V. Naidich, Kontaktnie Yavdeveya V, Metallicheskih Rasplavov, Nonkova Dumka, Kiev, 1972, p. 159 (In Russian).
61. G.V. Samasonov, I.F. Prydko and L.F. Prydko, Electronnaya Lokalizatsia Tverdom Tele, Nauka, Moscow, 1976 (In Russian).
62. E.W. Collings, 'Physical Metallurgy of Titanium Alloys', ASM, Ohio, 1984, p. 131.
63. H.W. Rosenberg, in 'The Science Technology and Application of Titanium', Eds. R.I. Jaffee and N.E. Promisel, Pergamon Press, Oxford, 1970, p. 851.
64. C.J. Smithells (ed.), 'Metals Reference Book', Butterworths, London, 1976, p. 426.
65. Z. Lev and G. Welsch, Met. Trans. A, Vol. 19A, April, 1988, 1121.
66. Same as Ref. 64, p. 879.
67. J.C. Chesnutt, C.G. Rhodes and J.C. Williams, in 'Titanium and Titanium Alloys', Ed. M.J. Donachie, Jr., ASM, Ohio, 1982, p. 160.
68. M.A. Greenfield, C.M. Pierce and J.A. Hall, in 'Titanium Science and Technology', Eds. R.I. Jaffee and H.M. Burte, Plenum Press, New York, 1973, p. 1734.

